Dtsch. Entomol. Z. 70 (2) 2023, 261–282 | DOI 10.3897/dez.70.102952

PENSOFT

für Natur MUSEUM FÜR NATURKUNDE BERLIN

An "American" silkmoth endemic to Himalayas, part I: life history and natural distribution of *Antheraea compta* Rothschild, 1899 (Lepidoptera, Saturniidae)

Zhengyang Liu[1]

1 *Zhangdian District, Zibo, Shandong Province 255000, China*

https://zoobank.org/DCDDAA33-01C1-4E9B-9B5B-B579BA37D008

Corresponding author: Zhengyang Liu (saturniidae@qq.com)

Academic editor: Wolfram Mey ♦ **Received** 3 March 2023 ♦ **Accepted** 8 June 2023 ♦ **Published** 4 July 2023

Abstract

Females of the uncommon *Antheraea compta* Rothschild, 1899 were collected at the natural habitat in the Tibetan Sub-Himalayas, descendants of which were reared on *Quercus yunnanensis* (Fagaceae) successfully, with all the preimaginal instars recorded morphologically. Correlated characters revealed a close relationship between this taxon and New World *Antheraea* spp., suggesting more attention and protection towards this key species is necessary in the future.

Key Words

chaetotaxy, ecoregion, evolution, Kachin, Meghalaya, morphology, protection, *Quercus*, SEM, silkworm, *Telea*, Tibet

Introduction

Species of *Antheraea* Hübner, 1819 have long been known in the history of sericulture as excellent sources for non-mulberry silk (Peigler 1993). Research surrounding the genus has always been a focus in Lepidoptera, occupying most of the scientific works on the family Saturniidae around the world because of their spectacular appearances and considerable economic benefits. After a systematic review, Nässig (1991) proposed to classify these silkmoths into three subgenera, i.e., *Antheraea*, *Antheraeopsis* Wood-Mason, 1886 and *Telea* Hübner, 1819. Textiles called Chinese tussah (from *Antheraea pernyi* (Guérin-Méneville, 1855)), Japanese tensan (from *Antheraea yamamai* (Guérin-Méneville, 1861)) and Indian tasar (from *Antheraea paphia* (Linnaeus, 1758)) make the subgenus *Antheraea* the center of attention, while the golden muga silk (from *Antheraea assamensis* (Helfer, 1837)) produced in Sub-Himalayas renders *Antheraeopsis* famous (Peigler 2020). The venerable polyphemus moth (*Antheraea polyphemus* (Cramer, 1775)) within *Telea* is a cultural icon in American entomology. From southern Siberia to the Indonesian islands, from central Europe to the Japanese archipelago, the subgenus *Antheraea* occupies almost all the humid broad-leaved forests from temperate to tropical Eurasia. *Antheraeopsis* flies in Asia only south of the level of Qinling Mountains, but in any case, populations within these two subgenera are all entirely limited to the Palearctic-Indo-Malayan regions. The main habitats of *Telea* are in the Nearctic-Neotropical realms, but one putative member, namely *Antheraea compta* Rothschild, 1899 (Fig. 1), is endemic to the northeastern part of the Indian subcontinent (Peigler 1999), this disjunct distribution considered one of the core mysteries in saturniid evolution.

The original type series of *A. compta* was stated to be from "Khasia Hills, Assam, 8 ♂♂, no ♀ [*sic*]", regarded from the beginning to be an adelphotaxon allied to *A. assamensis* within *Antheraeopsis* (Rothschild and Jordan 1899). Such judgment may have been based largely on the superficial features, especially the similar eyespots and the shared natural habitat. Subsequently, Rothschild and Jordan (1901) provided a color photo of a male *A. compta* and supplemented "The ♀ is similar to the ♂, but has a shorter and broader forewing [*sic*]". Watson (1912: pl. 2) first

Copyright *Zhengyang Liu*. This is an open access article distributed under the terms of the Creative Commons Attribution License (CC BY 4.0), which permits unrestricted use, distribution, and reproduction in any medium, provided the original author and source are credited.

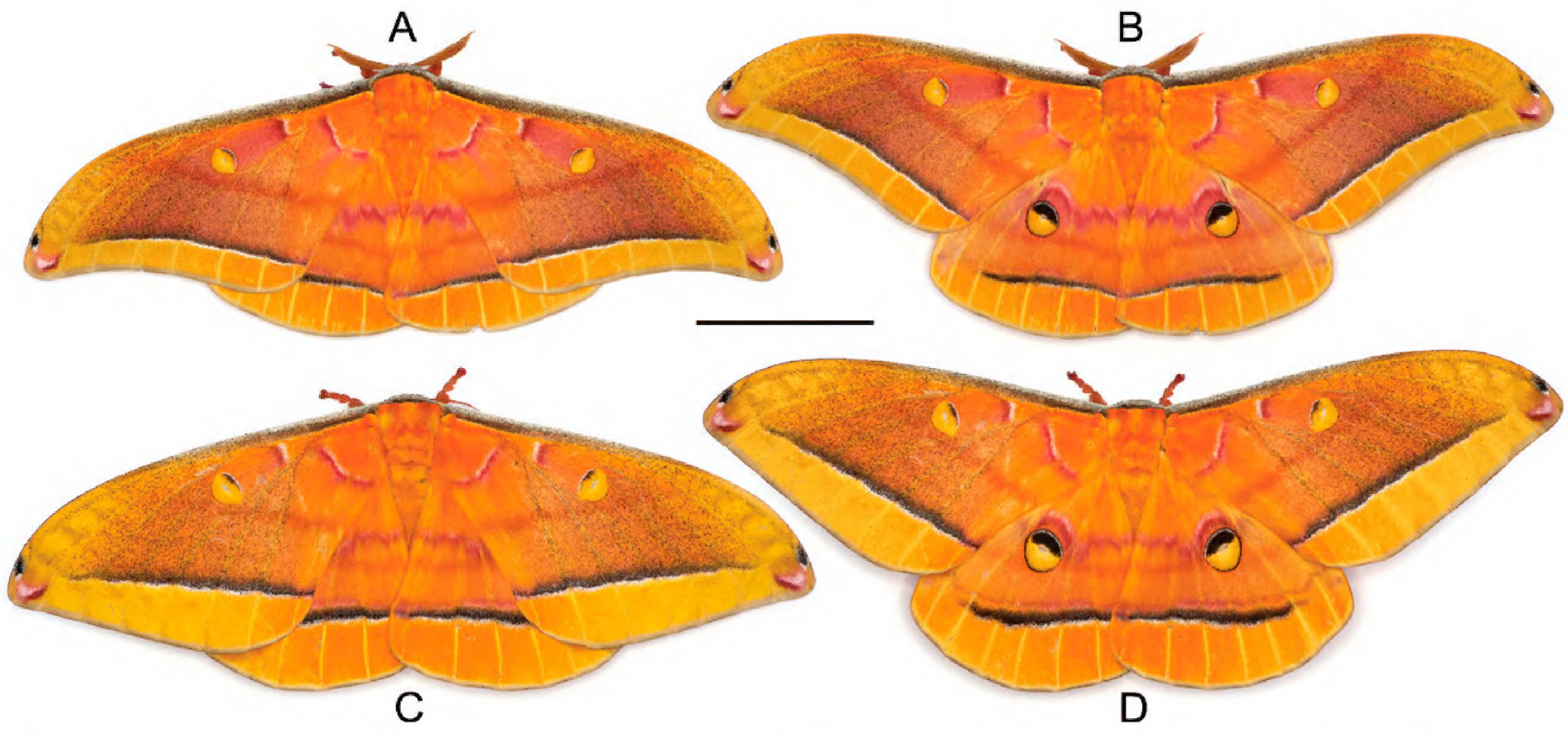


Figure 1. Living adults of *Antheraea compta*, dorsal views. **A.** ♂, calm condition; **B.** ♂, frightened condition; **C.** ♀, calm condition; **D.** ♀, frightened condition. Scale bar: 4 cm.

illustrated the female, captured at the type-locality. Packard (1914: 197) cited this taxon without additional comments, while Conte (1919: 14–15) and Seitz (1926–1928: 511) continued to associate *A. compta* with *A. assamensis*. The first entomologist who recognized the problem was Bouvier (1936: 167) who definitively stated that there is a fairly high morphological similarity between the male genitalia of Himalayan *A. compta* and Central American *Antheraea godmani* (Druce, 1892), especially their three-lobed valvae, although he did not transfer the former into his checklist for *Telea*. After a comparison with *A. polyphemus*, Lemaire (1978: 207) further acknowledged the strong homology with *A. compta* about male genital structures, a taxonomic opinion recognized in more recent works (Nässig 1991; Nässig et al. 1996; d'Abrera 2012: 126–127; Naumann and Löffler 2015), but Meister (2011: 144) still regarded *A. compta* as a member of the gerontogeous subgenus *Antheraea*, while Paukstadt et al. (2000, 2003) suggested that the issue requires further clarification. Arora and Gupta (1979: 30) drew the venations of Indian *Antheraea* spp. and noticed the forewing R1 [radial vein 1] of *A. compta* ("Maghalaya, Cherra Punji, 1220–1524 m., 1 ♂, 24.vii.1931 [*sic*]") is relatively longer than that of *A. assamensis*, with a more medial arising point on the anterior margin of the discal cell, but those two authors did not discuss the New World taxa.

Except for Khasi Hills, specimens of *A. compta* have also been collected from "Assam, Jaintia Hills… 12 Juill. 1922 [*sic*]" and recorded by Bouvier and Riel (1931: 53), subtropical forests of the two areas were formerly in Assam, but belong to Meghalaya today (Gupta 2000); furthermore, a male moth from the adjacent Hahim of Assam was reported by Peigler (1999). Bryk (1944) published a more distant record of specimens mentioned as *A. compta* discovered at "Kambaiti, 2000 m, 9.VI–17.VI [*sic*]" [Kanpaikti Sub-Township, Kachin State] in northeastern Burma by the entomological expedition of René Malaise in 1934 (specimens viewed by Richard S. Peigler in Stockholm in 2005, personal communication to Liu from Peigler on 31 Aug. 2022). The third core population of the species inhabits southeastern Tibet (Fig. 2), first noted as "Motuo [Metok] County… 2120 m, VII.2013 [*sic*]" by Naumann and Löffler (2015) (a separate species? see below), and in 2019, living material from the same ecoregion was unsuccessfully reared on *Quercus* sp. (Fagaceae), died in L_3 without detailed description (Naumann and Nogueira 2021), but suggested the caterpillars "fit very well with typical habitus of *Telea* larvae [*sic*]".

The above mentioned moths were collected at upland mid-altitudes (ca. 1000–2500 m) in the height of summer, basically June-July (Bouvier and Riel 1931: 53: "11 Déc. 1903 [*sic*]" possibly invalid), so the species is considered to be a strictly univoltine Himalayan flyer. It must be admitted that specimens of *A. compta* are rare in collections worldwide, so obviously knowledge of its complete preimaginal stages is of great significance for our understanding of the evolutionary history of the genus *Antheraea* or even the family Saturniidae.

Material and method

INSIZE 1108-150C 0-150 mm / 0.01 mm (± 0.02 mm) was used to measure general lengths. XINGYUN FA1204E 120 g / 0.0001 g (± 0.0002 g) for recording weights. BENETECH GM1365 (± 2 RH%; ± 0.3 °C) for recording air humidity and temperatures. BENETECH GM1020 (≤ 10000 Lux ± 3%; ≥ 10000 Lux ± 4%) for recording illuminances. PHILIPS TL 6W (UV-A, peak: 365 nm), was used for fluorescence photographs. All color figures were photographed by a NIKON D5500 with SIGMA 10–20 mm *f*/4–5.6 lens or LAOWA 60 mm *f*/2.8–22 lens. ZEISS GeminiSEM 360 was used for the SEM observations and photographs, based on sputter-coated samples of 2 ova, 6 L_1, 1 L_5, 1 L_6 and 1 cocoon of *A. compta*. The



Figure 2. The natural habitat of *Antheraea compta* in southeastern Himalayas. Mêdog County, Tibet Autonomous Region, China, 2122 m. 28 Jun. 2021.

sources of botanical and other zoological materials will be given in the corresponding paragraphs below.

Terms involving continuity in time or space, the corresponding numbers use the subscript format, including: $L_{1–6}$ = 1st–6th larval instars; $T_{1–3}$ = 1st–3rd thoracic segments; $A_{1–10}$ = 1st–10th abdominal segments.

Structures not having the above relationship between each other are cited: S = stemma [ocellus]; BaS = sensillum basiconicum; ChS = sensillum chaeticum; TrS = sensillum trichodeum; PlS = sensillum placodeum; CaS = sensillum campaniformium; DiS = sensillum digitiformium; StS = sensillum styloconicum. If necessary, ending with Arabic numerals (non-subscript) for coding (e.g., "S1", "ChS1"). Classification of the sensilla mostly consults some lepidopterous works, i.e., Dethier (1937, 1941), Schoonhoven and Dethier (1966), Grimes and Neunzig (1986a; 1986b) and Faucheux (1999: 247–280). Ryan (2002: 113–114) expressed that the term "chaetic" is applicable to thicker-walled bristles or spines, the word "trichoid" means slender and hair-like, and both can be used for chemo- or mechanosensilla (Zacharuk and Shields 1991; Keil 1999; Shields 2008), so they are sometimes hardly distinguishable externally. Schneider (1964) thought such definitions are strictly morphological, the former "distinguished by a specialized and flexible circular membrane at the base [*sic*]", and the latter "without any specialized basal cuticular ring serving as articulating membrane [*sic*]". In addition, the word "sensillum (sensilla)" is used in figures only for some specified structures which are borne on antennae, maxillary palpi, maxillary mesal lobes and labial palpi. Here are labelled other primary setae and pores on labrum, mandibles and maxilla-hypopharynx-labial complex into only "lateral (L)", "medial (M)", "dorsal (D)" and "ventral (V)" in figures, but does not rule out that they may have special sensory functions.

Larval chaetotaxy, described below as far as possible, follows the universal terminology named in earlier Lepidoptera publications, primarily based on Heinrich (1916), Gerasimov (1935) and Hinton (1946), with also the reviews by Chu (1956), Stehr (1987), Piao and Lee (1998) and Hasenfuss and Kristensen (2003). Additional works treating the standard setal coding of the family Saturniidae were consulted, of which Pease (1960), Heppner and Wang (1987) and Rougerie and Estradel (2008) are examples. The abbreviations of general areas are as follows: O = ocellar [stemmatal]; SO = subocellar [substemmatal]; F = frontal; AF = adfrontal; C = clypeal; G = genal [microgenal/midgenal]; A = anterior; V = ventral; SV = subventral; L = lateral; M = medial; XD = tactile dorsal (on the anterior margin of prothoracic shield and near the dorsal midline); D = dorsal; SD = subdorsal; MD = microdorsal [vertical]; P = parietal [posterodorsal]. Combined with these directional terms, Arabic numerals (non-subscript) and lowercase letters respectively code related primary setae and pores of the head (e.g., seta "SO1", pore "MDa"). The term "pore" for text below may appear to be depressed (pierce the cuticle, or not) or elevated. Further, the term "palpifer" is only used for the maxillae in this work, whereas "palpiger" is considered as a part of the labium, although some entomologists used the latter term within the maxillae (e.g., Peterson 1948: 119; Schoonhoven and Dethier 1966).

Nässig (1989) and Deml and Dettner (2002) classified saturniid scoli focusing on their basal morphology and functionality (secretions), but this article only divides related primary setae into the following four conditions expressed by Roman numerals on the setal map of T_1–A_{10} (Fig. 3); each of them is considered as a "term" for modifying singular or plural nouns, hyphenated with a general area abbreviation (e.g., seta(e) "D-I", chalaza(e) "D-I", area(s) "D-I"), distinguished in detail with final Arabic numerals (non-subscript) if necessary (e.g., seta(e) "D-I1", seta(e) "D-I2"):

I = For describing a single seta, or the structure/location in which it resides [uni-setal]. If used for the

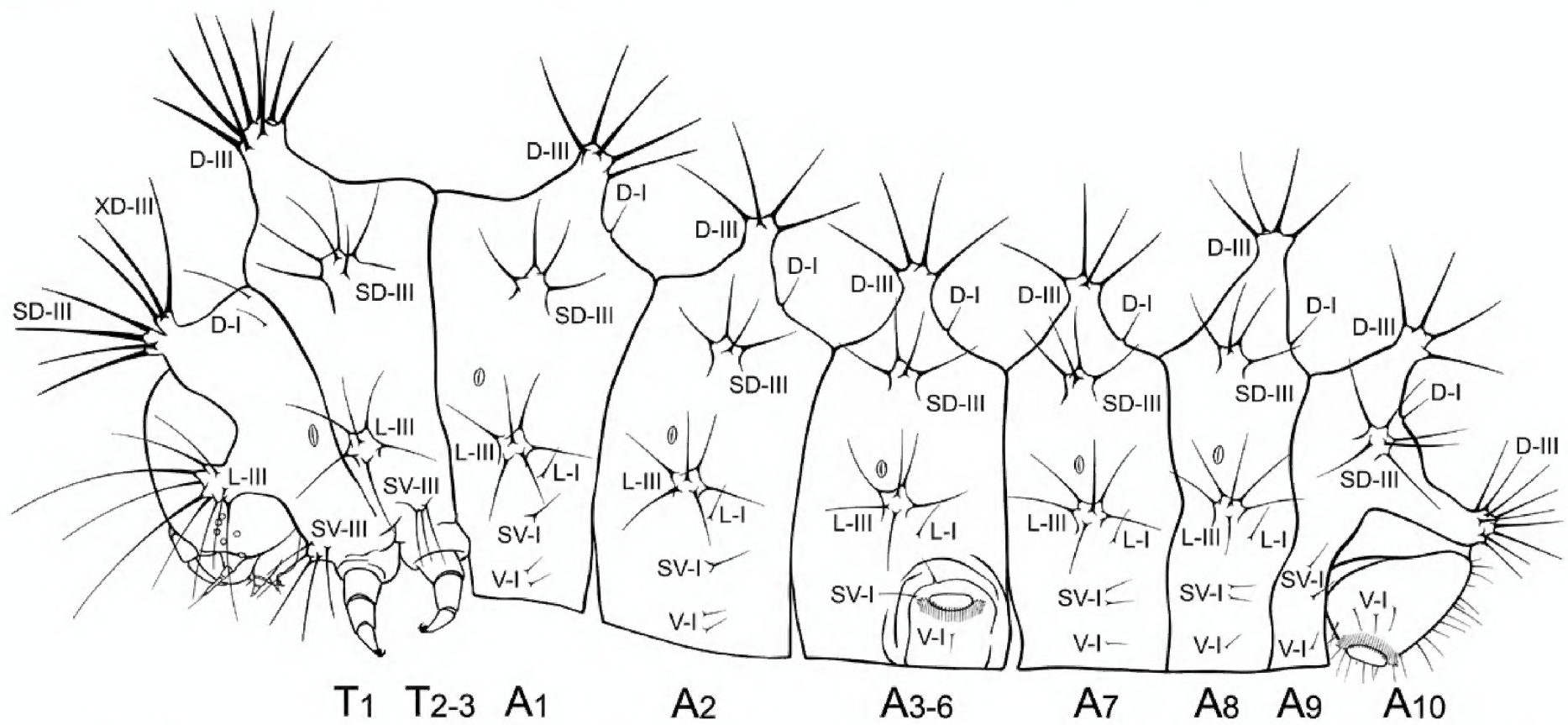


Figure 3. L_1 of *Antheraea compta*, the setal map, lateral view, with only the primary chaetotaxy coded. The setae of cephalic regions and legs $T_{1–3}$ are not shown, proleg A_{10} displays the mesal surface, the ventral midline constitutes the bottom margin of $A_{1–9}$.

plural, for example, several setae within the designated area, then each seta is treated as an individual existing independently which could be objectively distinguished from others.

II = For describing a pair of setae (n = 2), or the structure/location in which they reside collectively [bi-setal]. If used for the plural, for example, several setal pairs within the designated area, then each pair is treated as an individual existing independently which could be objectively distinguished from others.

III = For describing a cluster of setae (n > 2), or the structure/location in which they reside collectively [multi-setal]. If used for the plural, for example, several setal clusters within the designated area, then each cluster is treated as an individual existing independently which could be objectively distinguished from others.

IV = For describing uncertain condition on the designated structure/location [uni/bi/multi-setal].

Results

Morphology of preimaginal instars

Unless otherwise specified, numerical (metric) data was based on single normal individual in this chapter, and the fluorescence tests are only valid for naked eye vision.

Ova (Figs 4, 8A)

Tri-axial ellipsoid, ca. 3.71 mm (length) × 3.32 mm (width) × 2.18 mm (height) (Fig. 4A–D). The micropylar zone is relatively flat, the external formation of rosette is combined by polygonal imprints of follicle cells (Fig. 4F, G). Other areas of the exochorion covered reticular crests [chorionic sculptures], walls generally heighted in ca. 18.7–30.4 μm and widened to ca. 27.1–34.8 μm, the begirded regions shaped into irregular subcircles with comparatively smooth surfaces in most cases (Fig. 4E), but in the circumferential zone of the ovum (except the micropylar zone) (Fig. 4B, C), some of such fragments and their walls formed into special spongiform (Fig. 4H), decorated as darker color (Figs 4A, 8A). The aeropyles (widths = ca. 2.32–12.1 μm) dispersedly located at intersections of the network except the micropylar part (Fig. 4E). Aeropyle crowns (widths = ca. 16.6–37.9 μm) are not fully developed (incomplete or missing) and only localized to the vertices of the spongy polygons (Fig. 4I). The hydrophilic ovum shell is colored mostly opaque white under dry conditions, but becomes translucent after being sprayed with water causing the internal embryo to be visible (Fig. 4A), while the aeropyles are the major pathways for water desorption possibly (Fig. 4E). The chorionic interior is multihole mainly superimposed by lichen-like fillers (Fig. 4J), such minute lobes are hung loosely in more external (Fig. 4K), and stacked densely as multiple tiers in more internal (Fig. 4L). Chorionic thicknesses (excluding re-

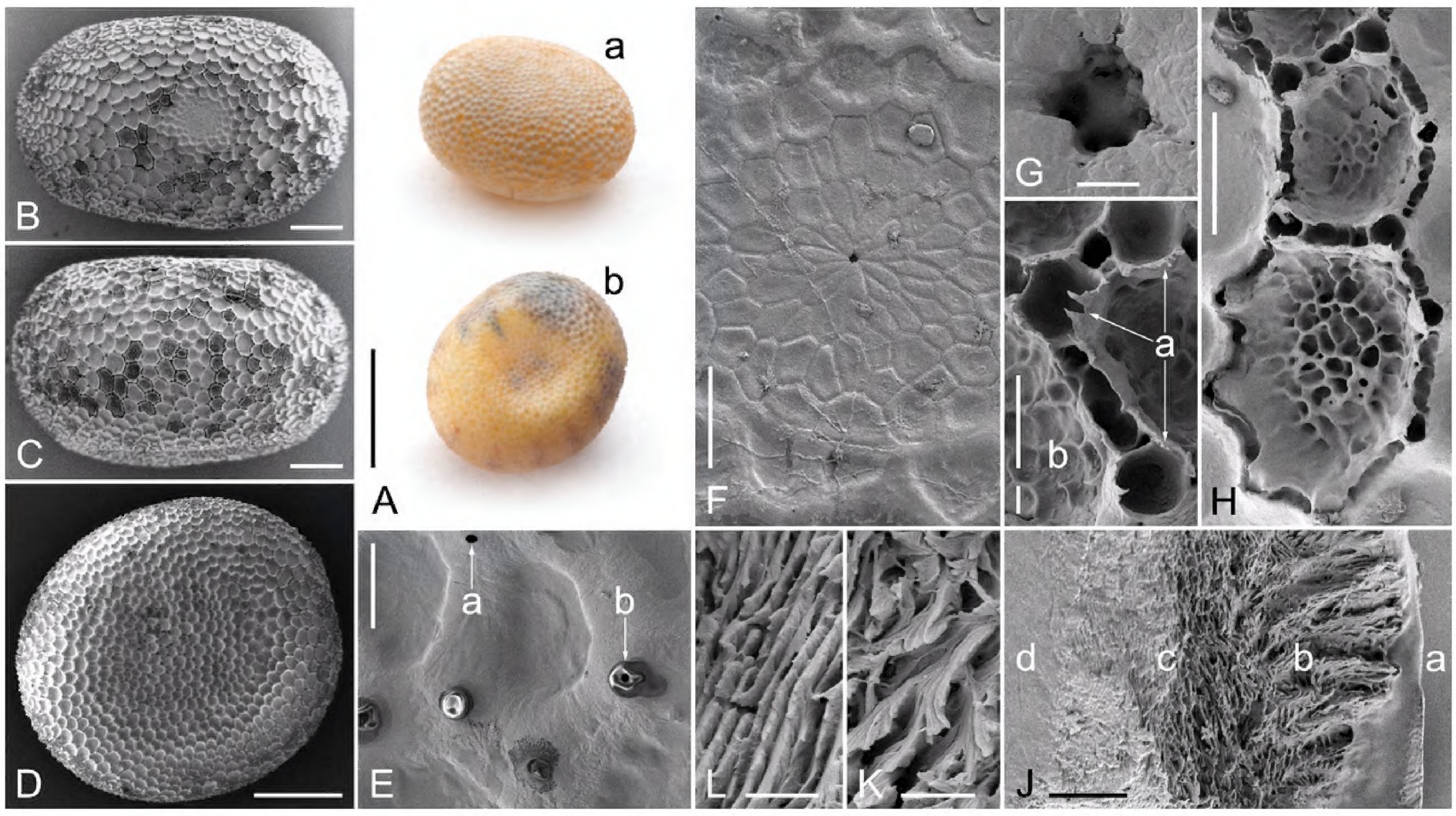


Figure 4. Ova of *Antheraea compta*. **A.** Fertilized ovum; a: dry condition; b: wet condition; **B–D.** Unfertilized ovum (the flat zones are critically sunken); **B.** Micropylar side of the circumferential zone; **C.** Non-micropylar side of the circumferential zone; **D.** Flat zone; **E.** Flat zone; a: dry aeropyle; b: wet aeropyle; **F.** Micropylar zone; **G.** Micropylar zone, the center; **H.** Circumferential zone, spongiform fragments and their walls; **I.** Circumferential zone, spongiform fragments and their walls; a: incomplete aeropyle crowns; b: spongiform structure; **J.** Chorionic cross section; a: exochorion; b: exo-fillers; c: endo-fillers; d: endochorion; **K.** Chorionic exo-fillers; **L.** Chorionic endo-fillers 2 μm. Scale bars: 2 mm (**A**); 500 μm (**B, C**); 1 mm (**D**); 40 μm (**E, I**); 5 μm (**G**); 2 μm (**K, L**); 100 μm (**F, H**); 10 μm (**J**).

ticular crests and micropylar zone) are ca. 44.3–48.2 μm. The glue secreted from adult accessory glands [colleterial glands] for affixing the ova is diluted into clear honey brown color, inconspicuously concentrated on the bottom external surface which contacts the vegetation; other areas seemed clean and without glue.

Larvae

L_1 (Figs 3, 5–7, 8A–C)

Head capsule is 1.78 mm width with shiny black appearance, whose anteclypeus is gray and longitudinally folded. Bearing 17 pairs of longer primary setae namely P1, P2, L1, AF1, AF2, F1, C1, C2, A1, A2, A3, O1, O2, O3, SO1, SO2 and SO3, they are pointed and with a smooth surface and sometimes slightly helical-shaped (Fig. 5A, D, E), seta P1 is the longest (length = 1.16 mm), seta F1 (length = 182.5 μm) is the shortest. There are 4 other pairs of minute primary setae (lengths = ca. 7.4–8.1 μm) erectly, i.e., MD1, MD2, MD3 and G1 which ended with rounded apexes (Fig. 5A, B, J). A total of 10 pairs of primary pores appeared on the head capsule, coded as Pb, La, AFa, Aa? [Pa?], Fa, Oa, Ob, SOa, MDa, and Ga (Fig. 5A–E), among them, the pores Fa (width = 21.1 μm), Ob (width = 16.6 μm) and SOa (width = 24.7 μm) are slight raised (e.g., Fig. 5L), other ones are flat-bottomed or bowl pits with widths of ca. 9.4–12.5 μm (e.g., Fig. 5K, M–P), the deepest depression is pore Ga. A case was found that the sites of pores Pb are asymmetric, i.e., in the same specimen, they are respectively located on the inferolateral and superolateral sides to setae P2, but the former condition is normal. In addition, a few secondary setae and pores could be asymmetrically observed in individuals. S1 (width = 47.7 μm), S2 (width = 46.3 μm), S3 (width = 58.9 μm), S4 (width = 50.3 μm), S5 (width = 48.1) and S6 (width = 46.7 μm) have multiporous surface (e.g., Fig. 5I), their anisotropic wrinkles have observed on dry exuviae and alcohol-preserved specimens (Fig. 5A), but unclear if living larvae have the same feature. S1 and S6 are flatter, whereas S3 is the most elevated.

The antennal sclerites are mostly dark maroon linked with light gray antacoriae. The 2nd antennal segment is multiporous and elongated peanut-shaped, whose lower part of the sclerotized wall is embossed with slight reticular crests forming dense polygons, its longish ChS1 (length = 372.2 μm) and ChS2 (length = 90.7 μm) dotted dispersedly with tiny wall-pores (more obvious on ChS2) and standing lateroapically (Fig. 6A–C). Of the segment, BaS1 is dorsoapical, BaS2 and BaS3 are ventroapical, CaS1 (width = 13.2 μm) is lateroproximal (Fig. 6D), CaS2 and CaS3 (widths = ca. 4.5–4.9 μm) are lateroapical. Relatively, the 1st and 3rd segments of antenna have fewer pores on the walls, the latter is implanted distal BaS4, BaS5, BaS6 and StS (Fig. 6B, C). Antennal BaS1, BaS2 and BaS4 showing fingerprint-like surfaces (lined pores) and rounded tips with similar lengths of ca. 20.2–25.4 μm, alike epicuticle also observed on BaS3, BaS6 and BaS5, but the former two owning varying degrees of forky apexes (BaS3 usually has 2–4 forks and asymmetrically presents in a specimen, BaS6 is always bifurcated) with respective maximum lengths of 15.6 μm and 8.7 μm, BaS5 is an elevated pimple in 5.8 μm height. The external surface of uniporous StS (length = 18.0 μm) is smoother, exhibiting sharp or uni/bis-papilliform terminals.

The labral anterior surface is sepia, shiny, arrayed primary setae L1, L2, L3, M1, M2 and M3 in pairs with plane ends, seta M2 is the longest with 204.4 μm length and other ones are ca. 84.7–178.5 μm. The primary pores Ma, Mb and Mc are ca. 9.5–16.11 μm widths, the sizes one by one incrementally (Fig. 5F). The labral posterior surface [epipharynx] is off-white principally but the mid-notch [groove] is sepia. Except the smooth margin, other area covered by white and short denticulations densely, exhibiting pointed and flatted setae M4, M5 and L4 (lengths = 82.9–93.4 μm), with a digitiform seta L5 in size ca. 56.8 μm (length) × 24.3 μm (width), they are aporous. Symmetrically paired pores Md, Me and Mf are obvious, the latter is the biggest up to 17.5 μm width, while other two are reduced to ca. 12.3–14.0 μm (Fig. 5G). Setae L1–5 and M1–5 are clear brown, pores Ma-f are campaniform.

Each mandible has 6 teeth (4 outer and 2 inner), primarily bears a pair of neighboring setae L1 (length = 295.9 μm) and L2 (length = 134.2 μm), with a pimple-like pore La (width = 27.8 μm) which is surrounded by dense subcircular pits. The posterior condyle [postartis] is a prominent smooth knob (Fig. 5F, H).

The weakly sclerotized cardo is nearly a semicircle, the stipes forms a "F" shaped sclerite whose longer margin is lying medially and the arm points to the lateral side, its anterior and posterior edges respectively array the primary setae L1 (length = 202.2 μm) and L2 (length = 213.3 μm). Setae M1 (length = 218.3 μm) and M2 (length = 90.2 μm) could be invariably found on the apical margin of the incomplete annular sclerites, separately belongs to the palpifer and the 1st maxillary palpal segment; the latter has a striate-wrinkled top and connecting with the maxillary mesal lobe [galea], their medial junction zone (facing to the hypopharynx) is membranous and placing many toothed setae (Figs 6E, 7A–C). The sclerotized walls encircling maxillary palpus and mesal lobe are distally multiporous, the apical membranes of the latter and the 2nd–3rd segments of the former are knot-wrinkled (Fig. 7B, G, I). Maxillary palpal CaS1–4 are lateral, thereinto CaS1 and CaS2 are pits while CaS3 (height = 1.8 μm) is elevated, but both forms are applicable to CaS4 (Fig. 7A, C, D, H). Each maxillary palpus ended with BaS1–8 (lengths = ca. 5.2–5.6 μm) which have rounded tips and many campaniform olfactory pores (Fig. 7G). Dorsal sensilla of the 3rd maxillary palpal segment are rough, PlS1, PlS2 and PlS3 in widths of ca. 5.4–7.2 μm always surround the lateral to proximal sides of DiS (length = 11.8 μm; widths = 6.6 μm), distal morphology of the latter is alterable with 2–4 slight apical forks in different individuals and sometimes showing a sagittal concave midline (e.g., Fig. 7E, F). Each max-

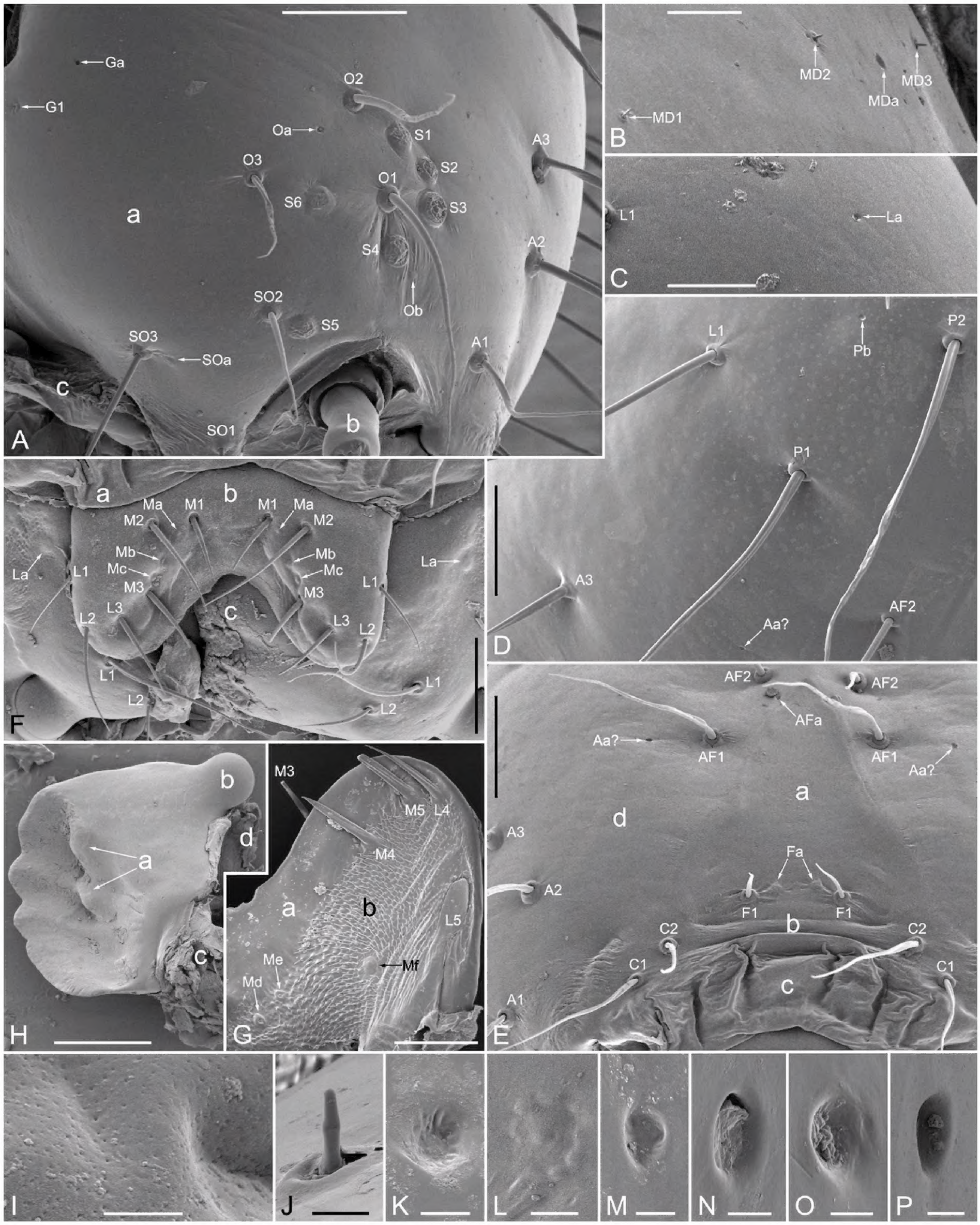


Figure 5. L_1 of *Antheraea compta*. **A.** Ventrolateral view; a: head capsule; b: antenna; c: cervacoria; **B.** Head capsule, superolateral view; **C.** Head capsule, lateral view; **D.** Head capsule, superofrontal view; **E.** Head capsule, frontal view; a: frons; b: clypeus; a + b: frontoclypeus; c: anteclypeus; d: other area; **F.** Mouthpart (partly), frontal view; a: anteclypeus; b: labrum; c: mandible; **G.** Labrum, posterior view [epipharynx]; a: the smooth marginal area; b: the hirsute area; **H.** Mandible, the inner surface; a: inner teeth; b: posterior condyle; c: adductor; d: abductor; **I.** The external surface of S3, vertical view; **J–P.** Primary seta and pores of head capsule; **J.** Seta MD3, lateral view; **K.** Pore Pb, vertical view; **L.** Pore SOa, vertical view; **M.** Pore Aa? [Pa?], lateroapical view; **N.** Pore MDa, lateroapical view; **O.** Pore La. lateroapical view; **P.** Pore Ga, lateroapical view. Scale bars: 200 µm (**A, D, E, H**); 50 µm (**B**); 150 µm (**C, F**); 80 µm (**G**); 2 µm (**I**); 6 µm (**J**); 5 µm (**K, N, P**); 15 µm (**L**); 7 µm (**M, O**).

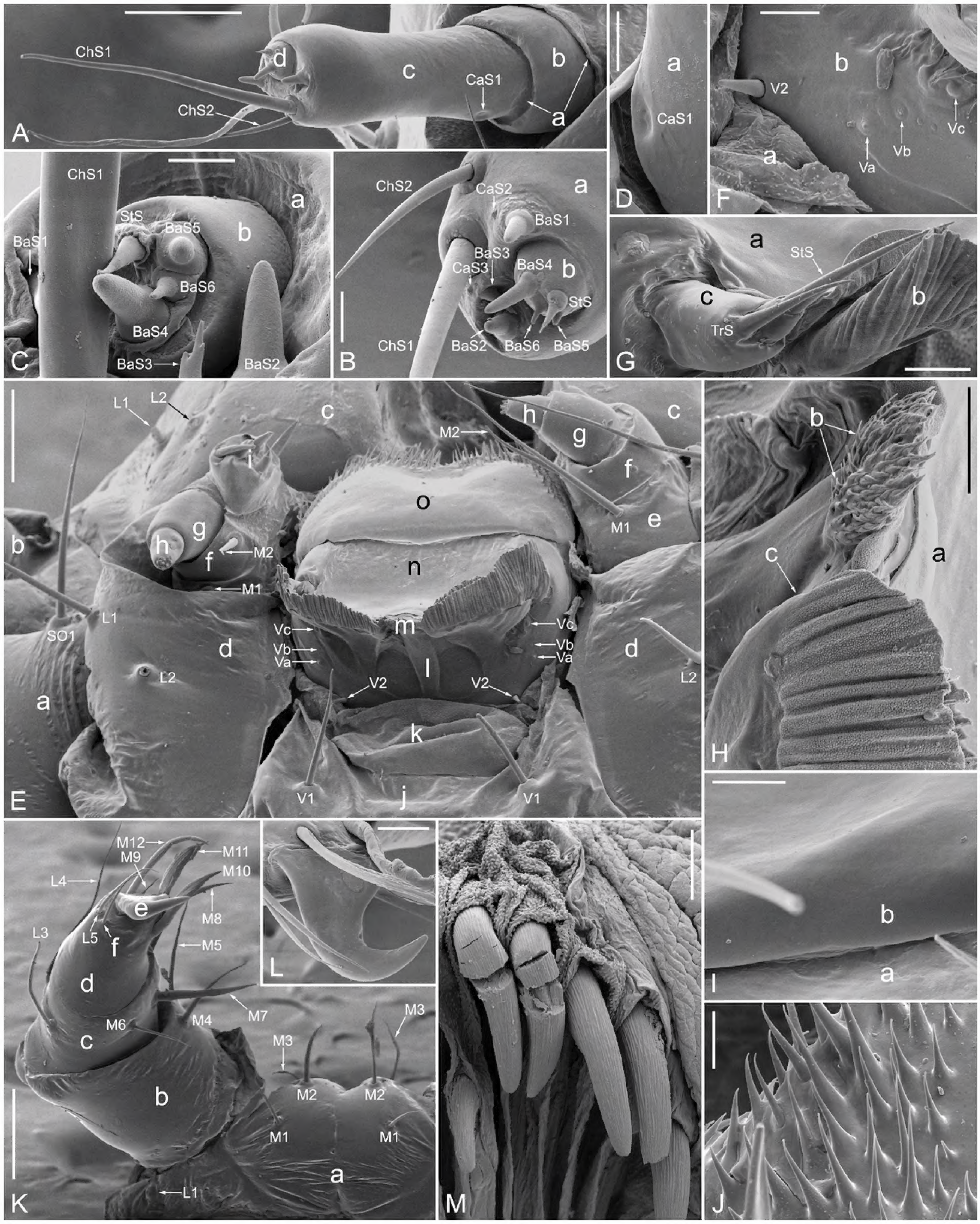


Figure 6. L_1 of *Antheraea compta*. **A–D.** Antennae. **A.** a: antacoriae; b–d: the 1st–3rd segments; **B.** a, b: the 2nd–3rd segments; **C.** a, b: the 2nd–3rd segments; **D.** a: the 2nd segment; **E.** Ventral view; a: head capsule; b: antenna; c: mandibles; d: stipites; e: palpifer; f–h: the 1st–3rd maxillary palpal segments; i: maxillary mesal lobe; j: postmentum; k: mentum; l: prementum (posterior); m: spinneret; n: prementum (anterior); o: hypopharynx; **F.** Ventrolateral view; a: mentum; b: prementum (posterior); **G.** Anterolateral view; a: prementum (anterior); b: the lateral lobe of spinneret; c: labial palpus; **H.** Lateral view; a: prementum (anterior); b: the medial lobes of spinneret; c: the lateral lobe of spinneret; **I.** Anteroventral view; a: prementum (anterior); b: hypopharynx; **J.** The lateral margin of hypopharynx (faces to the maxilla), lateral view; **K.** Legs T_1 (seta L2 is obscured), anterior view; a: coxae; b: femur; c: tibia; d: tarsus; e: pretarsus; f: secondary [subprimary?] seta; **L.** Pretarsus of leg T_1; **M.** Crochets of proleg A_4; ventral view;. Scale bars: 100 μm (**A, E**); 20 μm (**B, D, F–I, M**); 10 μm (**C, J**); 200 μm (**K**); 60 μm (**L**).

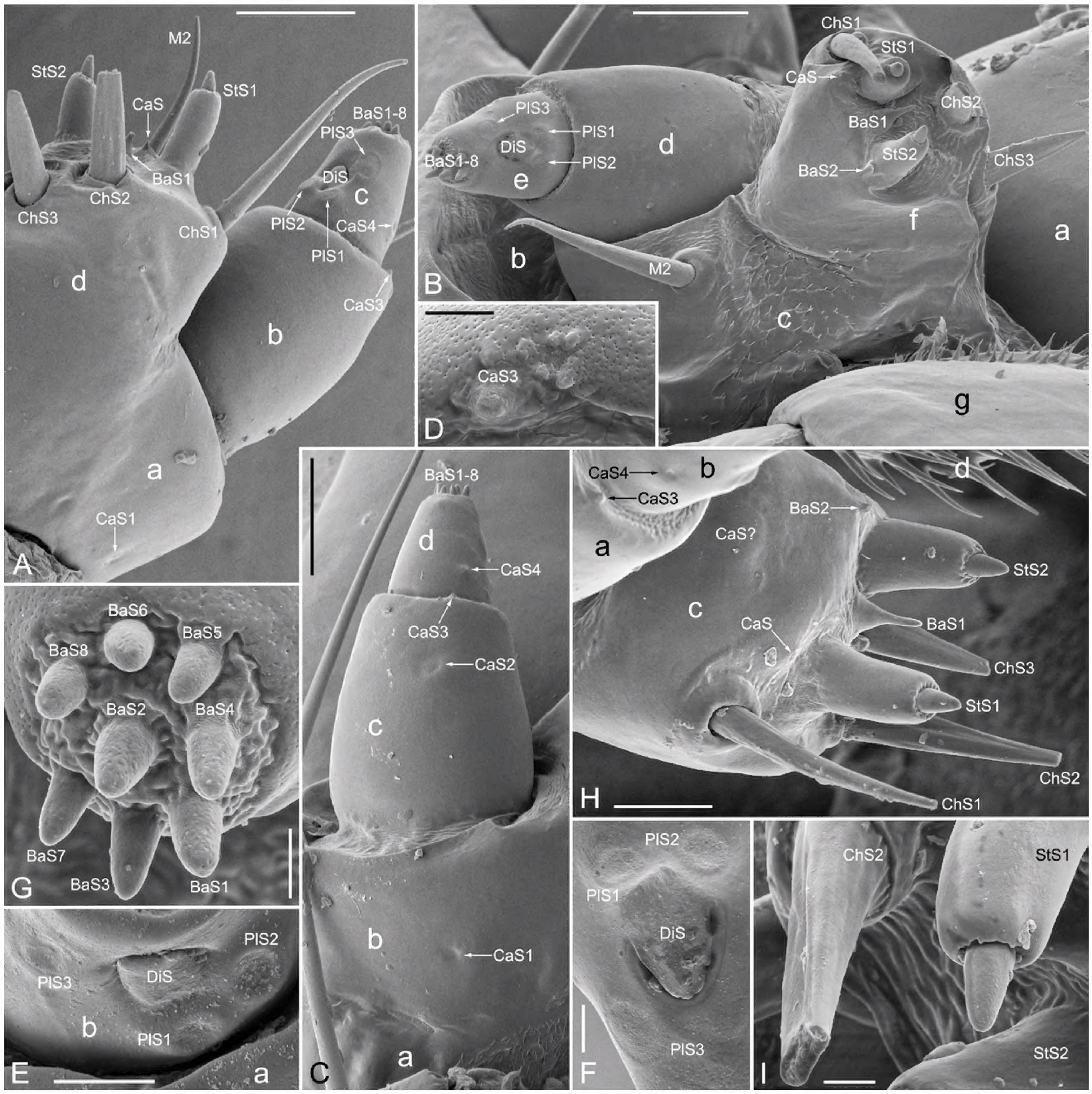


Figure 7. L_1 of *Antheraea compta*. **A.** Dorsolateral view; a–c: the 1st–3rd maxillary palpal segments; d: maxillary mesal lobe; **B.** Medial view; a: mandible; b: palpifer; c: the hirsute membranous zone between the 1st maxillary palpal segment and mesal lobe; d, e: the 2nd–3rd maxillary palpal segments; f: maxillary mesal lobe; g: hypopharynx; **C.** Lateral view; a: palpifer; b–d: the 1st–3rd maxillary palpal segments; **D.** Part of the apex of the lateral area of the 2nd maxillary palpal segment, apical view; **E.** Apical view; a, b: the 2nd–3rd maxillary palpal segments; **F.** Part of the dorsal area of the 3rd maxillary palpal segment; **G.** The apex of the 3rd maxillary palpal segment, apical view; **H.** Ventromesal view; a, b: the 2nd–3rd maxillary palpal segments; c: maxillary mesal lobe; d: hypopharynx; **I.** Part of the apex of the maxillary mesal lobe, medioapical view. Scale bars: 40 μm (**A–C**); 4 μm (**D, G**); 10 μm (**E**); 5 μm (**F, I**); 20 μm (**H**).

illary mesal lobe arranging flat-topped ChS1, ChS2 and ChS3 from the lateral to medial, they are multiporous but such perforations of the former are more obvious and on the latter two are thinner. The lengths of ChS1 are unstable and the measurements based on a single specimen are 54.7 μm and 84.9 μm, ChS2 and ChS3 are special chisel shaped and ca. 37.8–41.2 μm lengths. The elevated basal columns of StS1 and StS2 are relatively smooth (less pores) with lengths of ca. 23.6–27.8 μm, their terminal dome topped cones are morphologically look like the maxillary palpal BaS1–8, but lengthened to ca. 8.3–9.0 μm (Fig. 7I) with finer pores. For each maxillary mesal lobe, BaS1 is terminally uniporous and tapered (length = 14.2 μm), while BaS2 is rough and reduced to a small wart (height = 3.4 μm), and, an indeterminate shaped CaS (in the same larva, respectively crater-like and spine-like) was fixedly observed on the ventroapical margin and located close to StS1 (Fig. 7B, H). On the ventral area is a very large subcircle forming a slight protrusion with weak wave-like margins marked as CaS? (Fig. 7H), it is

aporous and seems to only be observed at specific angles with certain light conditions, and its function is unclear.

The postmentum [submentum] is smooth and membranous largely, the proximolateral sclerite [submentales] is adjacent with the maxillary cardo, primary seta V1 (length = 104.1 μm) is close to the border with the mentum, the latter is a semicircular membrane covered by minute noncellular processes (Fig. 6E, F). The prementum [stipulae] is lyre-shaped with most areas membranous, but a crescent sclerite is inlaid proximally of the posterior surface which abutted with the mentum, primary seta V2 (length = 14.6 μm) is smooth and rounded. Campaniform pores Va, Vb and Vc are ca. 4.9–5.4 μm widths, always present on the posterolateral area of the prementum (Fig. 6F). The cleft spinneret is fleshy and semitransparent, whose linguiform medial lobes [glossae] are hirsute and the pliciform lateral lobes [paraglossae] are fine-grained surfacely (Fig. 6G, H). The distance between the two labial palpi is 238.8 μm, each of them dotted with many micropores but more remarkable on the lateral TrS (length = 47.2 μm) and medial StS, the basal and setal parts of latter are respectively 16.5 μm and 68.0 μm lengths (Fig. 6G). The distal area of the hypopharynx is smooth but the posterior lingua is covered by numerous spines (Fig. 6I, J).

The setal map and related statistics are provided here (Fig. 3; Table 1). Grounded with bright yellow on T_1–A_{10} generally but the cervacoria and venter are lower saturation. The dorsal area of T_1 dotted with three black spots, one shown betweenthe pair of scoli XD-III and other two exhibited on the dorsolateral respectively. Each of T_2–A_8 decorated two black dots along the dorsal midline, these segments have also lateral black stripes between the levels D and L. Level SV of A_9 lying a big black dapple on each side (divided along the dorsal and ventral midlines), while the anal shield, and the lateral surface of each proleg A_{10} appearing as a large black patch shaping nearly semicircular, the latter structure distributed 13–18 bristles on the posterior to ventral margin. All thoracic and abdominal setae are translucent, to be the longest on scoli L-III of T_1. Scoli XD-III, D-III, and SD-III bear stout brown to black setae and the latter two have significantly elevated bases; other chalazae/scoli are developed with white setae. A pair of scoli D-III are medially fused on A_8, whose fusional characteristic is similar to the case of scoli XD-III and SD-III on the anterior margin of prothoracic shield on each side. Spiracle T_1 is the largest whereas spiracles $A_{1–8}$ are relatively small, all brownish colors. The paired sclerites of coxae are unclosed annular shaped and medially fused on T_1. Coxal setae L1 and L2 are respectively located on the antero/postero-terminal areas of the sclerite, other primary setae coded as M1, M2 and M3. The femur apically bears setae M4 and M5; each tibia has 6 setae labeled M6, M7, M8, M9, L3 and L4. On the top of the tarsus, setae M10, M11 and M12 are widened with slight longitudinal crests, seta L5 is a weak hair (Fig. 6K). A thick basal lobe is displayed on the pretarsus (Fig. 6L), sometimes there are secondary [subprimary?] setae occurring on legs $T_{1–3}$

Table 1. L_1 of *Antheraea compta*, a quantity statistic of chalazae/scoli of the single side (divided along the dorsal and ventral midlines), and the numbers of primary setae borne on each them (in brackets). The "?" means inconclusive.

Structures\Segments	T_1	$T_{2–3}$	A_1	A_2	$A_{3–6}$	A_7	A_8	A_9	A_{10}
Scoli D-III		1(8)	1(5)	1(4)	1(4)	1(4)	1(4)	1(4)	1(9?)
Chalazae D-I	2 (1)		1(1)	1(1)	1(1)	1(1)	1(1)	1(1)	
Scolus XD-III	1(3–4)								
Scoli SD-III	1(4)	1(6)	1(4)	1(4)	1(4)	1(4)	1(4)	1(6)	
Scoli L-III	1(8–10)	1(6)	1(6)	1(6)	1(6)	1(6)	1(6)		
Chalazae L-I			1(1)	1(1)	1(1)	1(1)	1(1)		
Scoli SV-III	1(4–5)	1(3)							
Chalazae SV-I			1(1)	1(1)	2–3(1)	2(1)	2(1)	2(1)	
Chalazae V-I			2(1)	2(1)	1(1)	1(1)	1(1)	1(1)	4?(1)

(e.g., Fig. 6K). The plantae of prolegs are rosybrown in lateral view, each of them arranged dark maroon crochets in uniserial heteroideous mesoseries, the numbers are 23–27 ($A_{3–6}$) and 26–29 (A_{10}), such hooks have solid insides and longitudinally plicated epicuticle (Fig. 6M).

L_2 (Fig. 8D–F)

The primary chaetotaxy and related fusions are unchanged to L_1. The head capsule (width = 2.61 mm) turned into sepia color with darker ocellar area. The antennal sclerotized parts are sienna connecting with golden antacoriae, the labrum, anteclypeus and frontoclypeus are bronzed. The cervacoria is lemon, the integumentary ground color of thorax-abdomen is largely pure or yellowish green but T_1 is always paler, the prothoracic shield (with scoli XD-III and SD-III) is gradually changing to light yellow with aquamarine scoli L-III. Chalazae SV-I of $A_{1–2}$ and scoli SV-III and are blue to yellow-green, other scoli L-III, SD-III, and all scoli D-III owning ultramarine to blueviolet bases in smooth, but the proximal halves of the latter two borne on T_2–A_8 have shiny silvery appearance, the maximum size always showing on scoli SD-III of $A_{2–7}$. Some setae are elongated to form clubbed tips which displayed on scoli XD-III of T_1, scoli D-III of T_2 (sometimes $T_{2–3}$) and $A_{2–9}$, as well as on all scoli SD-III and L-III, such special bristles lengthened on scoli D-III of T_2 to be longer than any others. Since this larval instar, secondary hairs beginning to obviously emerge from the cephalic regions and the venter of T_1–A_{10}, accompanied by the harder observing on chalazae D-I, L-I, V-I and partial SV-I. Spiracles are surrounded by amber integumentary edges. The sclerites of legs $T_{1–3}$ are sepia, the distolateral surfaces of proleg bases of $A_{3–6}$ developed many black dots with secondary setae, while prolegs A_{10} also stretched multidirectionally their marginal bristles. The lateral plate of each anal proleg is dyed with posterior ochre, central black and anterior yellow (sometimes displaying only the former two colors), the latter two colors usually corresponding multi-pitted surfaces, the feature similarly arises in the yellowish triangular area of the anal shield. The plantar colors of prolegs $A_{3–6}$ and A_{10} are the same as L_1, but the crochets rowed into uniserial homoideous mesoseries with the quantities of 26–30.

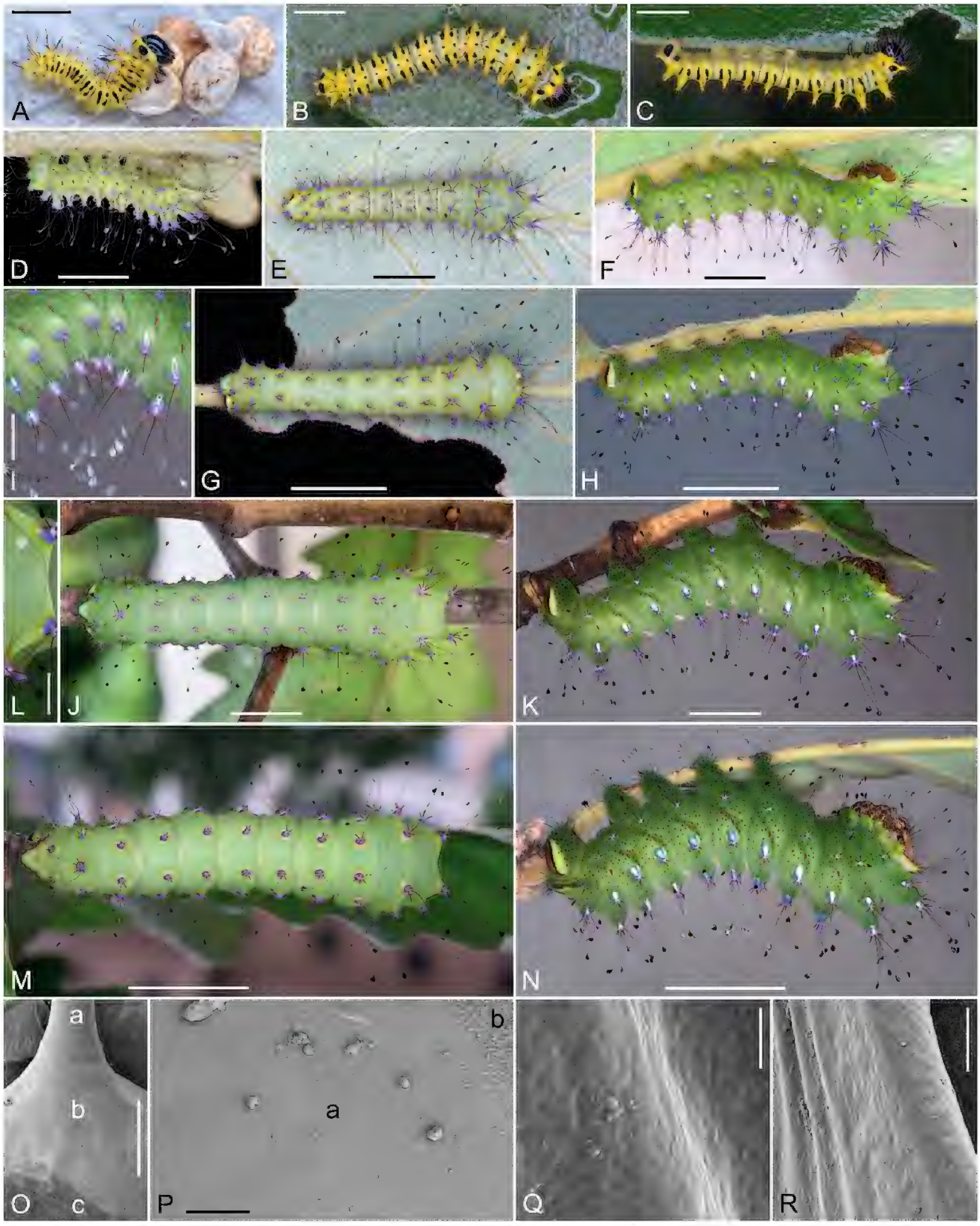


Figure 8. $L_{1\ 6}$ of *Antheraea compta*. **A.** L_1, newly hatched individual feeding on the eggshell, lateral view; **B.** L_1, drinking water, dorsal view; **C.** L_1, feeding on the edge of leaf (*Quercus yunnanensis*), lateral view; **D.** ♀, L_2, newly molted, lateral view; **E.** ♀, L_2, dorsal view; **F.** ♂, L_2, lateral view; **G.** ♀, L_3, dorsal view; **H.** ♂, L_3, lateral view; **I.** ♂, L_4, newly molted, $A_{2\ 8}$, lateral view; **J.** ♂, L_4, dorsal view; **K.** ♂, L_4, lateral view; **L.** ♂, the late period of the 4th pre-molting, the dorsal area of T_2, frontal view; **M.** ♂, L_5, dorsal view; **N.** ♂, L_5, lateral view; **O, P.** ♂, L_5, epicuticle of dry exuviae, the medial surface of scolus SD-III of A_1; **O.** a: spiny seta; b: shiny area; c: green integument; **P.** a: shiny area; b: green integument; **Q, R.** ♂, L_6, epicuticle of dry exuviae (sampling from cocoon), the clubbed setal apex of scolus D-III of T_3; **Q.** Centeral area; **R.** Marginal area. Scale bars: 3 mm (**A–C, I, L**); 5 mm (**D–F**); 1 cm (**G, H, J, K**); 2 cm (**M, N**); 200 µm (**O**); 30 µm (**P**); 4 µm (**Q**); 20 µm (**R**).



Figure 9. L_6 of *Antheraea compta*. **A.** ♂, lateral view; **B.** ♂, dorsal view; **C.** ♂, frontal view; **D.** ♂, posterior view; **E.** ♂, anal prolegs, lateral view; **F.** ♂, lateral margin of anal shield, dorsolateral view; **G.** ♂, head and T_{1-2}, anterolateral view; **H.** ♂, spiracle T_1, vertical view; **I.** ♂, legs T_{1-3}, ventral view; **J.** ♂, proleg A_{10}, ventral view; **K.** ♂, ventral view; a–c: A_{8-10}; d: sexual gland; **L.** ♀, ventral view; a–c: A_{8-10}; d: sexual gland; **M–T.** Latero-medioapical views; **M.** ♀, scolus D-III of T_2; **N.** ♀, scolus D-III of A_6; **O.** ♀, scoli D-III of A_8 (medially fused); **P.** ♀, scolus SD-III of A_6; **Q.** ♀, scolus SD-III of A_9; **R.** ♀, scolus L-III of A_6; **S.** ♂, scolus SV-III of T_3; **T.** ♂, chalaza SV-I of A_1. Scale bars: 2 cm (**A, B**); 1 cm (**C, D**); 5 mm (**E, G, I**); 2 mm (**F, M–T**); 1.5 mm (**H**); 2.5 mm (**J–L**).

L_3 (Fig. 8G, H)

General morphology close to L_2, but the head capsule is paler and widened to 3.73 mm. The flash basal parts have enlarged the volume further on scoli SD-III of $A_{2\text{-}7}$, especially. Supplemented long setae with club-like apexes on scoli D-III of T_3–A_1, as well as on chalazae SV-I of $A_{1\text{-}2}$ and scoli SV-III. Dense coryneform bristles initiating to present on the posterior zones of the middorsal $A_{2\text{-}6}$, colored as yellow vividly; they are minute and cross a transverse row combined by longer and pointed setae in the same color but borne on the anterior zones of $A_{3\text{-}7}$. Tricolored lateral plates of prolegs A_{10} observed in most of L_2 now shared in all individuals. More secondary hairs are exhibited principally on ventral integument. Some of them are based on dollar spots, such dots originating since L_2 are now widely distributed to level L, gradually colored from black to light brown. The marginal setae of A_{10} are pronouncedly elongated and orientated to the posterior side. The numbers of 50–55 crochets arranged as biordinal mesoseries on each planta.

L_4 (Fig. 8I–L)

The macroscopic pattern is essentially same as L_3, but the 5.47 mm width head capsule begins to appear more yellowish in proportions, mainly enriched on its ventrolateral and frontal zones, but the dark sepia strip ornamented on ocellar areas are still visible. The color of cervacoria is more vivid, slanted, parallel dark olive-green streaks arising between the levels SD and L of $A_{1\text{-}8}$. For T_2–A_{10}, the venter is clearly darker than dorsa, the dense dark spots are developing to the level SD with some secondary hairs, and the coxal apexes of legs $T_{2\text{-}3}$ are colored lightly like T_1. The clubbed setal apexes already occur on the longer bristles on prolegs, starting from this instar, each lateral plate of anal prolegs shows a very minute black dot on the yellow tint area with relatively fixed position, and each lateral margin of the anal shield formed into vitreum, enveloping an internal dark brown band. Plantar crochets are still biordinal mesoseries but increased to numbers of 54–60. Take L_4 as an example, for a fresh larva or during the pre-molting, the oblate setal tip could be seen white translucent, whereas the silver-reflective zones of scoli are transparent just after ecdysis but fully colored after approximately about 18–22 hours (Fig. 8I, L).

L_5 (Fig. 8M–P)

Head capsule (width = 7.33 mm) is paler distinctly, but the distribution patterns of colors are basically the same as L_4. The cephalic setae are more strongly developed, the dotted integument reaching the level D and all the secondary hairs turned into brownish to black with longer sizes. Parallel oblique stripes lying around spiracles $A_{1\text{-}8}$ are more evident, each spiracle is outlined by pale aquamarine margin. Scoli XD-III and SD-III on each side of prothoracic shield are highly fuse to be a unified base outwardly. The band inlaid inside the vitric margin of anal shield is now darker. The shining silvery bases of scoli D-III of T_2–A_9, and SD-III of T_2–A_8 are already spectacular (largest on scoli SD-III of $A_{2\text{-}7}$ still), their epicuticles are extraordinary smooth in stark contrast to the green integument, the latter is densely covered noncellular processes (Fig. 8O, P). Proleg plantae are surfaced with lateral dark gray and medial white with 61–64 crochets in biordinal mesoseries. Each of the lateral plates of prolegs A_{10} is constituted by the wrinkled bright yellow-green area, the smooth dark ochre posterior margin, and a narrow black stripe between the former two.

L_6 (Figs 8Q, R, 9, 10)

The final larval instar with giant body, head capsule is 10.32 mm width and the overall color pattern is near L_5 but more pallid (Fig. 9C, G). Combined with the high-saturation goldenrod cervacoria and the pale lemon coxae, the front margin of T_1 forms a bright yellow annular zone, which showed intensely fluorescent enrichment under the excitation by UV 365 nm (Figs 9G, 10B). Fluorescence was not detected in the flash bases with the clubbed setae (Fig. 10C), but weakly appeared on the yellow-green regions of the central anal shield and the lateral plates of prolegs A_{10} (Fig. 10D), the wrinkles of the latter are more obvious than those during the prior stage (Fig. 9E). Both scoli XD-III and SD-III have different numbers of primary setae during $L_{2\text{-}5}$ which appeared as short spines, but all of these are elongated into hair-like now (Fig. 9C, G). Similar to $L_{2\text{-}5}$, for all scoli, only partial setae on T_1–A_9 have clubbed tips (Fig. 9M–T), statistic on the single larva displayed that most setal quantities of the corresponding sites are same as L_1, but that on 12 scoli are decreased and 2 scoli are increased (Table 2). The rod-like part of the clubbed seta is smooth helical, the flaky end is paved by shallow pits densely but strongly reflection (Fig. 8Q, R). There is a significant difference in general integumentary color, i.e., 2 ♀♀ are more yellowish than 3 ♂♂, and the shiny scoli of females are tending to be purple-red but that of males look more purple-blue (Figs 9M–T, 10A). Observed the male sexual gland ["Herold's gland"] to be a slight mark localizing on ventral midline near to A_8/A_9 boundary (Fig. 9K), the female sexual gland ["Ishiwata's gland"] arising as two pairs of dots on ventral A_8 and A_9 (Fig. 9L). Distinguished from L_5, the dark spots are added to the middorsal area except the prothoracic shield, and the secondary hairs are increased on the whole body at present, but except the sizes, the glassy margins of anal shield as well as the spiracles are morphologically almost unchanged (Fig. 9F, H). Vesicular processes were observed on the distomedial areas of each tibia and tarsus, and all the medial setae (both primary and secondary) of legs $T_{1\text{-}3}$ form white thick spines (Fig. 9I), unfortunately, it lacked a leg observation for $L_{2\text{-}5}$. Plantae of $A_{3\text{-}6}$ and A_{10} bear 59–65 crochets within biordinal mesoseries (e.g., Fig. 9J). The liquid feces after feeding ended (all larval instars fed from *Q. yunnanensis*) is bronzed mucus (Fig. 10E), after that, 1 ♂ was recorded the weight as 14.77 g.

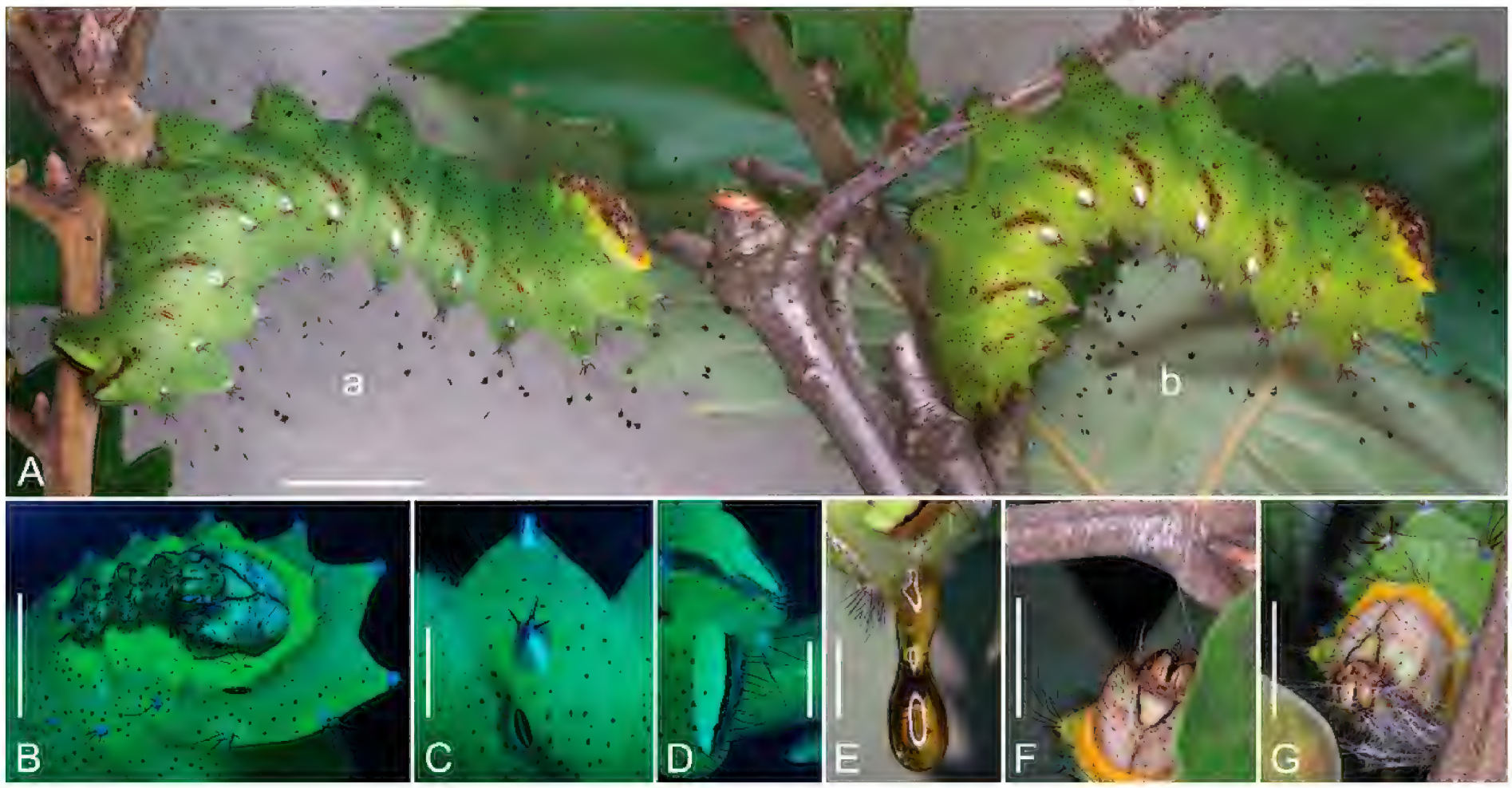


Figure 10. L_6 of *Antheraea compta*. **A.** Lateral view; a: ♂; b: ♀; **B–D.** ♂, under 365 nm UV; **B.** Head and T_1–A_1, ventrolateral view; **C.** A_7, lateral view; **D.** A_{10}, lateral view; **E.** ♂, the last defecation [liquid defecation] from A_{10}, lateral view; **F.** ♂, spinning the peduncle of cocoon; **G.** ♂, spinning the external part [floss] of cocoon. Scale bars: 2 cm (**A**); 1 cm (**B, F, G**); 5 mm (**C–E**).

Table 2. L_6 of *Antheraea compta*, a statistic based on primary chalazae/scoli which have clubbed setae, with the format "short spines + elongated hairs (how many clubbed ones)". The "<" is lower, the "=" is same, and the ">" is higher than the normal value of the corresponding locations during L_1 (see Table 1). Merged cells means the scoli are medially fused.

Segments\Areas	SV-I/III	L-III	SD-III	XD/D-III	XD/D-III	SD-III	L-III	SV-I/III
T_1	0 + 4(1) =	1 + 7(5) =	0 + 4(1) =	0 + 4(2) =	0 + 3(2) =	0 + 4(2) =	2 + 7(4) =	0 + 4(0) =
T_2	0 + 1(1) <	4 + 2(2) =	3 + 3(3) =	5 + 3(3) =	5 + 3(3) =	3 + 2(2) <	4 + 2(2) =	2 + 1(1) =
T_3	2 + 1(1) =	4 + 2(2) =	3 + 3(3) =	5 + 3(3) =	2 + 4(4) <	3 + 2(2) <	4 + 2(2) =	2 + 1(1) =
A_1	0 + 1(1) =	4 + 2(2) =	3 + 1(1) =	3 + 2(2) =	1 + 1(1) <	4 + 1(1) >	4 + 1(1) <	0 + 1(1) =
A_2	0 + 1(1) =	3 + 1(1) <	3 + 1(1) =	2 + 2(2) =	3 + 1(1) =	2 + 2(2) =	4 + 2(2) =	0 + 1(1) =
A_3		3 + 3(3) =	3 + 1(1) =	3 + 1(1) =	3 + 1(1) =	3 + 1(1) =	4 + 2(2) =	
A_4		3 + 2(2) <	3 + 1(1) =	3 + 1(1) =	3 + 2(2) >	3 + 1(1) =	4 + 2(2) =	
A_5		3 + 2(2) <	3 + 1(1) =	3 + 1(1) =	3 + 1(1) =	3 + 1(1) =	4 + 2(2) =	
A_6		4 + 2(2) =	3 + 1(1) =	3 + 1(1) =	3 + 0(0) <	3 + 1(1) =	4 + 2(2) =	
A_7		4 + 2(2) =	3 + 1(1) =	2 + 2(2) =	3 + 1(1) =	3 + 1(1) =	4 + 2(2) =	
A_8		3 + 2(2) <	3 + 1(1) =	2 + 2(2) =	2 + 2(2) =	3 + 1(1) =	3 + 2(2) <	
A_9			3 + 3(3) =	2 + 2(2) =	2 + 2(2) =	4 + 2(3) =		

Pupae (Figs 11, 12C)

The epicuticle is dark maroon to black except the translucent epicranial plate [frontoclypeus]. Females are larger (lengths: 3 ♂♂ = 40.58 mm, 39.64 mm, 38.68 mm; 2 ♀♀ = 42.63 mm, 44.48 mm) and heavier (weights of during overwintering diapause, measured on 06 Feb. 2023: 3 ♂♂ = 8.16 g, 7.46 g, 7.54 g; 2 ♀♀ = 9.29 g, 8.51 g) than males. The antennal margins in females are more flattened than males, the pair of antennae of the latter are not medially touching along the ventral midline, the maxillae and legs $T_{1\ 2}$ are visible in both sexes (Fig. 11C, E). Spiracles T_1 is gapped on the boundary of T_1/T_2 (Fig. 11F), spiracle $A_{2\ 7}$ are functional and large, but that of A_8 is closed as a remnant. A pair of forewing tubercles [adult spurs] is rendered on the dorsolateral areas of T_2 specifically (Fig. 11F). The biserial larval scoli D-III had been reduced to smooth vestiges on pupal stage, in only one case that such bulges on T_3–A_4 are obvious (Fig. 11H). The unsclerotized joints are junction zones between A_4/A_5, A_5/A_6, and A_6/A_7, the tip of A_{10} is rounded without cremaster (Fig. 11G). Genital pores are navel-shaped scars apertured midventrally for males (A_9) and females (A_8 [ostium bursae] and A_9 [ostium oviductus]) (Fig. 11B, D).

Cocoons (Figs 10F, G, 12)

Large (max-lengths without peduncles: 3 ♂♂ = 63.49 mm, 52.14 mm, 56.44 mm; 2 ♀♀ = 50.37 mm, 60.41 mm), single layered (thicknesses = ca. 0.37–1.16 mm) and fully closed (no pre-formed exit), the external part was woven by floss for attaching to leaves (Fig. 10G), the general shape is irregular polyhedron but the silky pupal cell is prolate spheroid. White colored in dry environment (weak fluorescence under UV

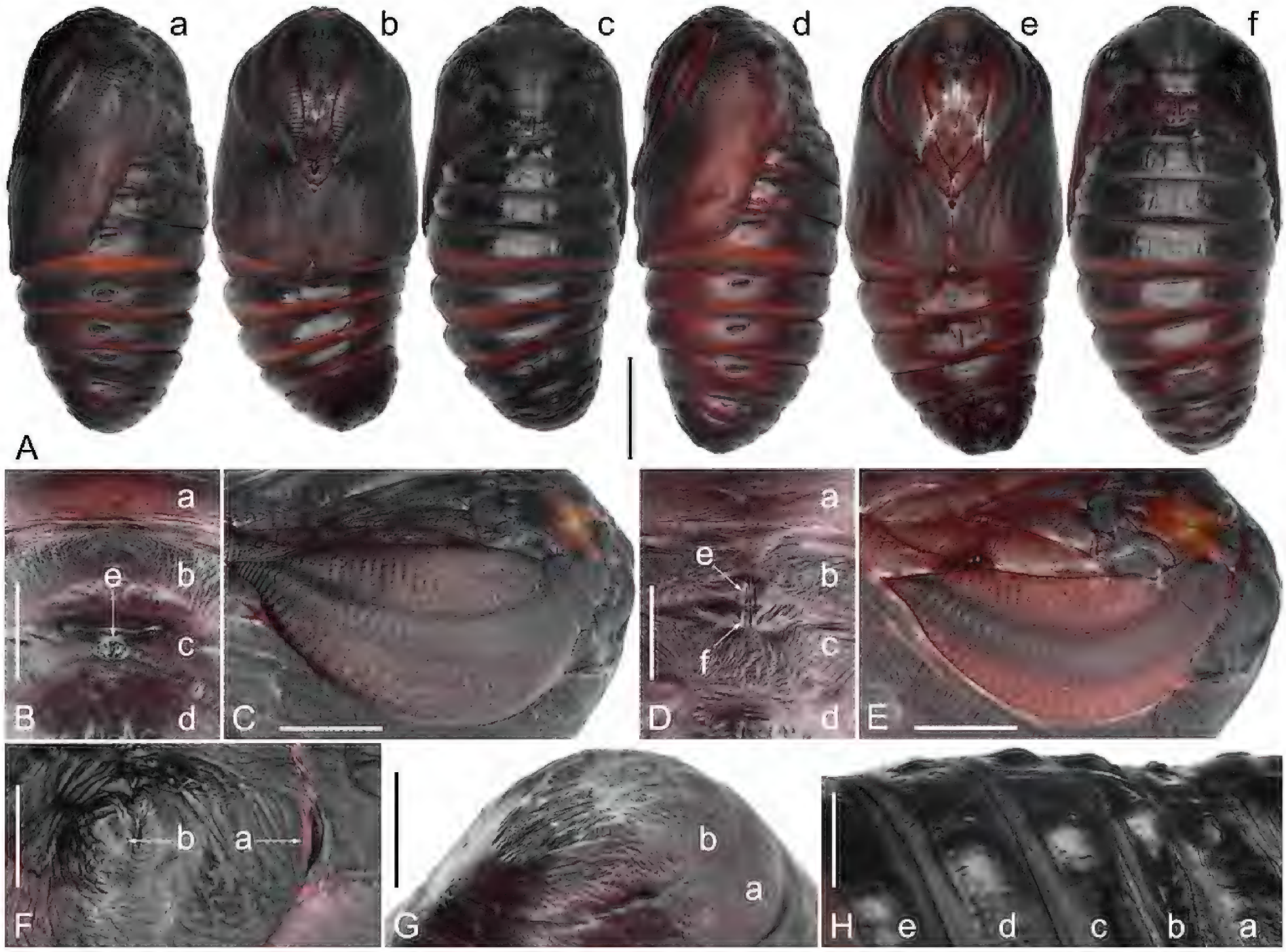


Figure 11. Pupae of *Antheraea compta*. **A.** a: ♂, lateral view; b: ♂, ventral view; c: ♂, dorsal view. d: ♀, lateral view; e: ♀, ventral view; f: ♀, dorsal view; **B.** ♂, ventral view; a–d: $A_{7\ 10}$; e: genital pore; **C.** ♂, head and $T_{1\ 2}$, ventrolateral view; **D.** ♀, ventral view; a–d: $A_{7\ 10}$; e, f: genital pores; **E.** ♀, head and $T_{1\text{–}2}$, ventrolateral view; **F.** ♂, $T_{1\text{–}2}$, dorsolateral view; a: spiracle T_1; b: forewing tubercle; **G.** ♂, posterolateral view; a, b: $A_{9\ 10}$; **H.** ♂, dorsolateral view; a–e: T_3–A_4. Scale bars: 1 cm (**A**); 2 mm (**B, D**); 5 mm (**C, E**); 3 mm (**F–H**).

365 nm, barely visible) but metamorphosing into brown tones in wet (fluorescence disappeared). 2 ♂♂ and 1 ♀ spun on erect vegetations with wide and loose peduncles of inferior structure (e.g., Figs 10F, 12A–C), 1 ♂ and 1 ♀ spun cocoons within fallen leaves and branches on the ground without peduncle (e.g., Fig. 12D). Each filament is a double-strand flat belt, wrinkles formed by longitudinal stretching could be observed on epi-sericin (Fig. 12F), the part of fibroin is combined by dense elongated fibers longitudinally to be almost non-porous within (less voids) (Fig. 12E). Microscopically surveyed three pieces (ca. 6.5–8.4 mm^2) of silk-layer sliced from random sites of a cocoon, showing the external surface is rougher, the filaments are ca. 83.8–94.4 μm wide and ca. 4.7–9.3 μm thick (Fig. 12H). The internal surface [pupal cell] is smooth and flat relatively, widths of the filaments are ca. 56.4–92.8 μm with the thicknesses of ca. 2.3–3.9 μm (Fig. 12I). Many crystals (mainly calcium oxalate) granulated from the prepupal discharge liquor are scattered or concentrated in the silk-layer (Fig. 12G), due to gravity, the precipitation is more obvious in the outer surface of the cocoon that lies closer to the ground.

Rearing report

During my first expedition on Tibetan Nyingchi, 1 ♀ of *A. compta* was collected on 28 Jun. 2021 from Mêdog 2122 m (Fig. 2), her 60 ova were hatched into 37 larvae in the experimental site in Kunming City of Yunnan Province, 1940 m, during mid Jul. to early Aug., these fresh L_1 rejected any Lauraceae, i.e., *Cinnamomum camphora*, *Cinnamomum burmannii*, *Machilus* spp., *Lindera* sp., *Neolitsea* sp., *Litsea pungens* and *Litsea populifolia*, moreover, *Magnolia delavayi* (Magnoliaceae), *Prunus cerasoides* (Rosaceae), *Salix babylonica* (Salicaceae) and *Liquidambar formosana* (Altingiaceae) were likewise not accepted. Finally, three individuals nibbled the leaves of *Quercus variabilis* and *Q. yunnanensis*, but only one grew into the 3rd pre-molting with the latter, and because it was reared outdoors without a cage, this larva was preyed upon by a *Myophonus caeruleus* (Aves: Passeriformes, Muscicapidae).

After the first failed attempt, I recaptured 3 ♀♀ adults with some males (Fig. 1) from the same natural habitat; during the rainy nights of 25–26 Jun. 2022, many large Quercus lamellosa were noticed at the site. Successively, 3 (coded as Gi, laid on 26 Jun.), 102 (coded as Gii, laid

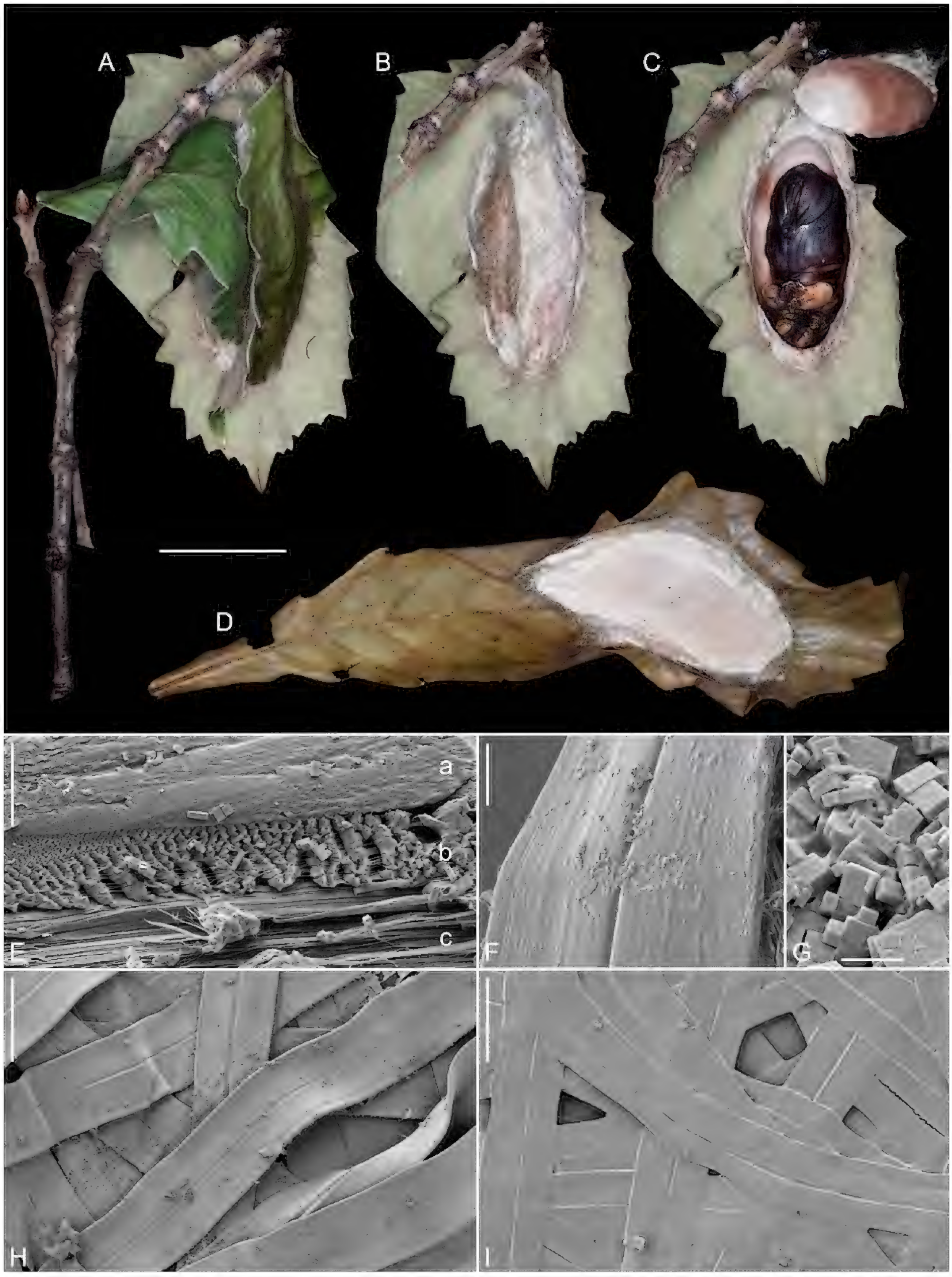


Figure 12. Cocoons of *Antheraea compta*. **A–C.** ♂, spun on the erect vegetation, lateral view; **A.** Original condition; **B.** Removed some leaves and branches; **C.** Opened; **D.** ♀, spun on the bottom of the net cage under a fallen leaf, lateral view [the underside]; **E.** ♂, filaments of the external part, cross sectional view; a: transverse [horizontal] plane; b: diagonal plane; c: sagittal plane; **F.** ♂, filament of the external part, vertical view; **G.** ♂, the crystals precipitated from the prepupal discharge liquor, vertical view; **H.** ♂, filaments of the external surface, vertical view; **I.** ♂, filaments of the internal surface, vertical view. Scale bars: 3 cm (**A–D**); 10 μm (**E**); 20 μm (**F**); 2 μm (**G**); 100 μm (**H, I**).

on 25 Jun.-01 Jul.) and 16 (coded as Giii, laid on 26–30 Jun.) eggs severally into paper envelopes. Each of Gi and Giii was oviposited naturally into a single tier without longitudinal accumulation, Gii was the same condition in the early period but later heaped up to lump because of larger quantity and lack of available space for adult abdomen. The material was brought back to the same site in Kunming indoor and then grouped on three mesh pieces, a cotton pad was placed below with interval ca. 1 cm, water sprayed the ova every day, the circumambient air was ca. 17–21 °C with ca. 80–95% RH. This method helped prevent water from accumulating around the eggs; excess water drained through the mesh openings to the cotton pad below, while the space between helped ventilate the bottom of the eggs to prevent mold.

At Beijing Time 06:00 to 16:00 every day, 3 larvae of Gi hatched on 13 Jul. (ovum period 17 days), 81 larvae of Gii hatched during 12–19 Jul. (ordered as: 10, 27, 12, 5, 15, 6, 5, 1; ovum period 17–18 days) and 14 larvae of Giii hatched during 13–18 and 20 Jul. (ordered as: 3, 4, 3, 1, 1, 1, 1; ovum period 17–18 or 20 days, but the last individual was unhealthy and died on the day of hatching). Newly hatched L_1 usually fed on eggshells preferentially. Checking unhatched material on 31 Jul., 17 ova of Gii and 1 ovum of Giii were devoid of embryonic development and shriveled; mature embryos had died in 4 ova of Gii and 1 ovum of Giii.

Fresh L_1 were moved to a semi-open balcony for rearing, without cage protection. The plant stems were inserted into the bottle filled with water, and the bottleneck blocked with paper towels to prevent larval drowning. Some newly hatched individuals did not bite the leaves of *Quercus schottkyana* and *Magnolia denudata* within two days, so all larvae were given *Q. yunnanensis*, which was readily accepted. These caterpillars had weak positive phototaxis, usually did not climb to the apex of host plant and did not exhibit gregarious behavior, but there were often 2–5 scattered L_1 on a single leaf. They rested on the undersides of the leaves and moved to the edges only when feeding, if a branch had fresh terminal buds and thick mature leaves, newly hatched larvae did not distinguish between them, as they are perfectly capable of gnawing on harder leaves, which is apparently related to their larger head with powerful mandibular adductors. Although they did not have strict requirements for air humidity during the larval stage (kept in ca. 64–98% RH), the temperature should not exceed 28 °C, otherwise the larvae will die in large numbers. When the environment reached 26 °C, they usually unclasped the legs T_{1-3} and prolegs A_{3-5} from host plant and suspended in air to enhance ventilation for heat dissipation. This may cause many larvae to fall to the ground. The whole larval stage accompanied a strong need for drinking water, and the leaves must be sprayed with water several times each day to ensure normal development of caterpillars, except on rainy days.

A. compta is a rather difficult species to rear in captivity with a very high mortality in L_1, in this study, only four individuals of Giii and five of Gii survived to the 1st pre-molting. However, two larvae within the latter group died during pharate and two died in early L_2. In the five surviving L_2, the individual "Giii1" was caged in outdoor and other four still fed semi-openly, until they cocooned respectively. Although the weather and nutritional conditions are identical, ontogenic time-consumptions are quite different in the same gender (Table 3).

Before entering each pre-ecdysis, larvae always moved away from their last feeding site. In late L_5 they cut the petiole to make the leaf fall to the ground or break it off completely to eliminate signs of feeding, which apparently helps to avoid some natural enemies which could find the caterpillar location by defoliation. Some individuals would sometimes entangle silk in selected locations to anchor themselves before shifting into apolysis state; such behavior was not consistent, but each of them always preferentially fed on their exuviae except the head capsule.

During L_{2-3}, larvae usually rested on the leaf midrib after a period of feeding of the lamina and secondary veins. For L_4 to medium L_5 they rested intermittently near the petiole and gradually nibbled along the midrib. Since late L_5, the weight only allowed the activities on branches, before feeding a new leaf, the larva often first bit a large pit on the petiole and then ate along the basal area, if necessary, gnawed more gaps on midrib for further folding the leaf apex closer to itself. For mature larvae, feeding behavior mostly occurred at night, probably to avoid detection by birds. A continuous observation on single L_6 was recorded for reference (Suppl. material 1).

All larval instars were sensitive to light, i.e., in resting states, they always faced toward the side where the illuminance is higher (Suppl. material 2), and this behavior would draw predators' attention to the bright yellow ring on the front of T_1, whose fluorescent was sufficient to indicate it plays a role in defensive warning. These caterpillars were extremely alert, and every slight shake would interrupt the feeding behavior. Under this state, larvae usually detached their legs T_{1-3} and prolegs A_3 (sometimes A_{3-4}) from the host plant, which may be an effective mimicry to make the lateral views more like leaves, sometimes clicking the mouthparts as a popping noise. The most alarmed individuals would swing from side to side, even triggering biting, whereas the special clubbed setae may help to enhance the spatial scope of tactile cue

Table 3. Developmental data of different individuals of *Antheraea compta*, fed from *Quercus yunnanensis*.

Stages\Codes	Giii1, ♂	Giii2, ♂	Giii3, ♂	Giii4, ♀	Gii1, ♀
Oviposited	30 Jun.	27 Jun.	28 Jun.	28 Jun.	25 Jun.
Hatched into L_1	17 Jul.	14 Jul.	15 Jul.	15 Jul.	12 Jul.
1st pre-ecdysis	27 Jul.	25 Jul.	26 Jul.	26 Jul.	23 Jul.
Molted into L_2	29 Jul.	27 Jul.	28 Jul.	28 Jul.	25 Jul.
2nd pre-ecdysis	05 Aug.	07 Aug.	08 Aug.	08 Aug.	06 Aug.
Molted into L_3	07 Aug.	09 Aug.	10 Aug.	10 Aug.	08 Aug.
3rd pre-ecdysis	14 Aug.	16 Aug.	18 Aug.	18 Aug.	17 Aug.
Molted into L_4	16 Aug.	18 Aug.	20 Aug.	20 Aug.	19 Aug.
4th pre-ecdysis	23 Aug.	26 Aug.	28 Aug.	30 Aug.	28 Aug.
Molted into L_5	26 Aug.	29 Aug.	31 Aug.	01 Sep.	31 Aug.
5th pre-ecdysis	05 Sep.	10 Sep.	14 Sep.	15 Sep.	17 Sep.
Molted into L_6	09 Sep.	15 Sep.	18 Sep.	19 Sep.	21 Sep.
Feeding ended	03 Oct.	09 Oct.	12 Oct.	16 Oct.	23 Oct.
Spun cocoon	04 Oct.	11 Oct.	13 Oct.	17 Oct.	24 Oct.

(Suppl. material 3). Even so, no secretions exude from the scoli under stimulated conditions, and no urticating reaction was detected on human skin after touch.

Larvae never left the host plant voluntarily if the leaves were plentiful. However, they quickly climbed or fell to the ground after feeding ended [liquid defecation] (happened at night usually), whereupon they were caged with upright living vegetation and dead leaves at the bottom for observation. Almost all individuals moved restlessly for about 24 hours before choosing a spinning location. The species undoubtedly constructs cocoons away from the host plant in the wild, either in low shrubs under the oak canopies or in the leaf litter on the ground.

The flight time in the natural habitat and captivity and reproductive behavior of adults will be recorded and published after the fresh adults emerge from existing pupae.

Discussion and conclusion

This article provides the first report of the complete life history of the enigmatic *A. compta*, whose lateral stripes of mature larvae are a feature close to that of North American *Antheraea oculea* (Neumoegen, 1883) (Tuskes et al. 1996: pl. 6; Lampe 2010: 121) and *A. polyphemus* (Bouseman and Sternburg 2002: 51; Hall 2021), the scale and distribution of the shiny silver spots closely resemble those in the Mexican *Antheraea montezuma* (Sallé, 1856) and *Antheraea meridiana* Naumann & Nogueira, 2021 (Paukstadt and Paukstadt 2020; Naumann and Nogueira 2021), while the tricolored lateral plate of anal proleg of Neotropical *A. godmani* (Nässig et al. 1996; Goossens et al. 2015) is similarly shared in *A. compta*. These observations preliminarily suggest that Himalayan *A. compta* should be assigned to the subgenus *Telea*.

Due to L_1 rejecting *Q. schottkyana* in captivity, it is inferred that *Q. lamellosa* is observed in the Tibetan habitat, and more cycle-cup oaks may not be the correct host plants to *A. compta*, namely the section *Cyclobalanopsis*. Additionally, in the eastern Himalayas, native specimens *Quercus lodicosa*, *Quercus lanata*, *Quercus engleriana*, *Quercus semecarpifolia*, *Quercus aquifolioides*, *Quercus gilliana*, *Quercus rehderiana* and *Quercus senescens* within the section *Ilex*, as well as *Quercus acutissima* of the section *Cerris* were also identified in recent works (Zhou and Sun 1996; Denk and Grimm 2009; Yang and Zhou 2015: 130; Lahiri et al. 2017), the three sections have been confirmed to form a monophyletic subgenus *Cerris* (Denk et al. 2017; Hipp et al. 2019). Because of the observed rejection of *Q. variabilis* (a single larva reluctantly ate a small gap, but did not continue), its sister taxon *Q. acutissima* would probably also be rejected. There is currently no experimental result on infrasubgeneric *Ilex* so it is uncertain whether *A. compta* can partially accept some species of the subgenus, but probably, *Q. lodicosa* and *Q. lanata* would be accepted as foods by such caterpillars; the former tree is common in southeastern Tibet and the latter is dominant from Mêdog to Tengchong County, Yunnan (bordered with Myanmar Kanpaikti), all having humid mid-altitudinal distributions (Zhou et al. 1995). In any case, the above species are clearly distinguished from *Q. yunnanensis*, a deciduous oak within the subgenus *Quercus*. Another roburoid white oak *Quercus griffithii* is widely known in northeastern India (Negi and Naithani 1995: 50–53; Singh et al. 2009; Singh et al. 2015), likewise naturally occurring in mountains from northern Yungui Plateau to sections of Indochina (Huang et al. 1999; Menitsky 2005: 47–49), with a high probability to be a primary host to *A. compta* at the corresponding biotopes.

A. assamensis is a well-known Lauraceae feeder in the wild (Seidel and Peigler 2018; Devi et al. 2021) but accepted beech (Lampe 2010: 358) and oak (Crotch 1956: 55) in captivity. Interestingly, the current known hostplants of *A. godmani* are limited to oaks (Meister 2011: 148), while *A. compta* is also oligophagous and feeding on certain *Quercus* only. This means that the empty cocoons collected from Assam soalu trees *Litsea monopetala* and then sent to Peigler (1999) were actually spun by muga silkworms. Therefore, Jolly's (1981) conclusion that "*A. compta* is almost identical with *A. assamensis* [*sic*]" is completely incorrect, while native Indian material for study of chromosomes (Gupta and Narang 1981) and silk (Luikham et al. 2017) using the former name but based on Lauraceae host plants are surely misidentifications to *A. assamensis* or its sister species *Antheraea castanea* Jordan, 1910. In fact, no Indian author has ever provided an adult image to prove the true identity of so-called "*A. compta*", except Arora and Gupta (1979) who described a pinned male from the British India period. In recent years, there have been a few indigenous records from the country but limited to only checklists without reliable morphological description and often confusingly called "wild muga" or "oak tasar" (e.g., Bhatia et al. 2010; Devi et al. 2011; Kumar et al. 2016; Gogoi and Goswami 2016; CSB 2018; Marepally 2018: 4; Boro and Borah 2020; Kumar et al. 2020; Keisa et al. 2022). This confusion suggests that the current population of the species may be nearly extirpated because virtually no local researchers have actually collected *A. compta*. Coincidentally, in works in which illustrated moth photographs corresponding to the scientific names, no specimen of *A. compta* was recaptured in recent surveys of northeastern India (Gogoi et al. 2014; Kakati and Chutia 2009; Kalita and Dutta 2014; Lalhmingliani 2015; Sondhi et al. 2021a) or even its type-locality Meghalaya (Shangpliang and Hajong 2015a, 2015b), whereas also does not turn up in the long-term monitoring of the Himalayas and Indian subcontinent (Shubhalaxmi 2018; Chandra et al. 2019; Sondhi et al. 2021b). To date, no Chinese publications included this species, and no records from Bhutan, Nepal and Uttarakhand are available, whereas Schüssler (1933: 175) added Sikkim to the distribution without supporting data.

Actually, the moths flying in southeastern Tibet were separated taxonomically from Meghalaya *A. compta*, the former was named *Antheraea discata* Naumann & Löffler, 2015, whose type locality is the same as the origin of my material. Unfortunately, the authors of *A. discata*

overlooked the study of specimens from mountainous Burma, and although they discovered some morphological and COI differences between Mêdog and Khasi Hills, the Myanmar samples are still crucial in resolving the phylogenetic relationships in this case. Unlike the natural barrier of the Assam Valley, the mountains of Sagaing-Kachin are connected to the Shillong Plateau and Himalayas, making it a logical corridor for the ancestral colonial activity of these moths. This suggests that the "species boundary" of *A. discata* is possibly fuzzy (transitional or gradual) or even not able to be located. Therefore, this paper rejects to use the name subjectively and treats it as "data-deficient" temporarily, however, it does not imply any effective taxonomic (synonymous) treatment for this taxon here. There is still a possibility in the future that the three ecoregional populations will be accepted as different species or subspecies to form a complex; the Sub-Himalayan genus *Sinobirma* Bryk, 1944 is a known case (Rougerie et al. 2012).

At present, the sources of published specimens of *A. compta* are localized within the following three restricted ecoregions of Indo-Malayan realm, the zoning based on Dinerstein et al. (2017):

- Meghalaya subtropical forests (Rothschild and Jordan 1899; Rothschild and Jordan 1901; Bouvier and Riel 1931: 53; Arora and Gupta 1979; Peigler 1999; Naumann and Löffler 2015).
- Northern triangle subtropical forests (Bryk 1944).
- Eastern Himalayan broadleaf forests (Naumann and Löffler 2015; Naumann and Nogueira 2021; this article).

Diverse evidence stresses the importance and necessity for conservation of wild *A. compta* in the current situation. As one of the central clues regarding the evolutionary history of the economically important genus *Antheraea*, its ecological and taxonomic significance is critical.

Larval feeding preference and morphological characters shared by the montane *A. godmani*, *A. montezuma* and *A. meridiana* with the Himalayan *A. compta* seemingly suggest that those Neotropical species are closer to the New World ancestor than are the Nearctic species (*A. polyphemus*, *A. oculea*). Three centuries of intense study of the genus *Antheraea* make more rigorous comparisons possible, and detailed phylogenetic studies on preimaginal morphologies and complete mitochondrial genomes of *A. compta* with related species are in preparation, to further confirm its evolutionary status.

Acknowledgments

I extend my sincerest thanks to the saturniidologist Dr. Richard S. Peigler (San Antonio), for his invaluable assistance with literature, manuscript review, and editing my English. His expertise in sericulture has greatly inspired and guided this article. Dr. Stefan Naumann (Berlin) reviewed the manuscript and offered related advice, along with fine editing by Dr. Wolfram Mey (Berlin). And I would like to thank Museum für Naturkunde (Berlin) for waiving the publication costs of this article.

References

Arora GS, Gupta IJ (1979) Taxonomic studies on some of the Indian non-mulberry silkmoths (Lepidoptera: Saturniidae: Saturniinae). Memoirs of the Zoological Survey of India 16(1): 1–63. [pls. 1–11]

Bhatia NK, Bhat MM, Khan MA (2010) Tropical tasar, utilization and conservation of natural resource for tribal development. The Ecoscan 1(Special Issue): 187–198.

Boro P, Borah SD (2020) Biodiversity of sericigenous insects in north-eastern region of India – a review. Journal of Entomology and Zoology Studies 8(4): 269–275.

Bouseman JK, Sternburg JG (2002) Manual 10: Field Guide to Silkmoths of Illinois. Illinois Natural History Survey, Champaign, 97 pp.

Bouvier EL (1936) Mémoirs du Muséum national d'Histoire naturelle (Nouvelle Série), Tome 3, Étude des Saturnioïdes normaux: Famille des Saturniidés. Éditions du Muséum, Paris, 354 pp. [12 pls.]

Bouvier EL, Riel P (1931) Catalogue des papillons sérigènes Saturnioïdes. In: Bouvier EL, Riel P (Eds) Essai de Classification des Lépidoptères Producteurs de Soie, 9e Fascicule. A. Rey, Lyon, 90 pp. [pls. 1–3]

Bryk F (1944) Entomological results from the Swedish expedition 1934 to Burma and British India. Lepidoptera: Saturniidae, Bombycidae, Eupterotidae, Uraniidae, Epiplemidae und Sphingidae, gesammelt von René Malaise. Arkiv för Zoologi 35A(8): 1–55. [1–6 pls.]

Chandra K, Kumar V, Singh N, Raha A, Sanyal AK (2019) Assemblages of Lepidoptera in Indian Himalaya through Long Term Monitoring Plots. Zoological Survey of India, Kolkata, 457 pp.

Chu HF (1956) The nomenclature of the chaetotaxy of lepidopterous larvae and its application. Acta Entomologica Sinica 6(3): 323–334.

Conte A (1919) Essai de classification des Lépidoptères producteurs de soie, 8e Fascicule. A. Rey, Lyon, 37 pp. [(pp. 6–42), 13 pls.]

Crotch WJB (1956) A Silkmoth Rearer's Handbook. The Amateur Entomologists' Society, London, 165 pp. [26 pls.]

CSB [Central Silk Board] (2018) Commercially exploited sericigenous insects of the world and their food plants. https://csb.gov.in/silk-sericulture/silk

d'Abrera B (2012) Saturniidae Mundi: Saturniid Moths of the World. Part 2. Goecke & Evers, Keltern, 178 pp.

Deml R, Dettner K (2002) Morphology and classification of larval scoli of Saturniinae and Hemileucinae (Lepidoptera: Saturniidae). Journal of Zoological Systematics and Evolutionary Research 40(2): 82–91. https://doi.org/10.1046/j.1439-0469.2002.00181.x

Denk T, Grimm GW (2009) Significance of pollen characteristics for infrageneric classification and phylogeny in *Quercus* (Fagaceae). International Journal of Plant Sciences 170(7): 926–940. https://doi.org/10.1086/600134

Denk T, Grimm GW, Manos PS, Deng M, Hipp AL (2017) An updated infrageneric classification of the oaks: review of previous taxonomic schemes and synthesis of evolutionary patterns. In: Gil-Pelegrín E, Peguero-Pina JJ, Sancho-Knapik D (Eds) Oaks Physiological Ecology. Exploring the Functional Diversity of Genus Quercus L. Springer, Cham, 13–38. https://doi.org/10.1007/978-3-319-69099-5_2

Dethier VG (1937) Gustation and olfaction in Lepidopterous Larvae. The Biological Bulletin 72(1): 7–23. https://doi.org/10.2307/1537535

Dethier VG (1941) The antennae of lepidopterous larvae. Bulletin of the Museum of Comparative Zoology at Harvard College 87(6): 455–507. [pls. 1–9]

Devi KI, Singh LS, Singh NI, Dutta K, Singh KC (2011) Biodiversity of sericigenous insects and their food plants in Manipur. The Ecoscan 5(1–2): 65–68.

Devi B, Chutia M, Bhattacharyya N (2021) Food plant diversity, distribution, and nutritional aspects of the endemic golden silk producing silkworm, *Antheraea assamensis* – a review. Entomologia Experimentalis et Applicata 169(3): 237–248. https://doi.org/10.1111/eea.13021

Dinerstein E, Olson D, Joshi A, Vynne C, Burgess ND, Wikramanayake E, Hahn N, Palminteri S, Hedao P, Noss R, Hansen M, Locke H, Ellis EC, Jones B, Barber CV, Hayes R, Kormos C, Martin V, Crist E, Sechrest W, Price L, Baillie JEM, Weeden D, Suckling K, Davis C, Sizer N, Moore R, Thau D, Birch T, Potapov P, Turubanova S, Tyukavina A, de Souza N, Pintea L, Brito JC, Llewellyn OA, Miller AG, Patzelt A, Ghazanfar SA, Timberlake J, Klöser H, Shennan-Farpon Y, Kindt R, Lillesø JPB, van Breugel P, Graudal L, Voge M, Al-Shammari KF, Saleem M (2017) An ecoregion-based approach to protecting half the terrestrial realm. Bioscience 67(6): 534–545. https://doi.org/10.1093/biosci/bix014

Faucheux MJ (1999) Biodiversité et unité des organes sensoriels des Insectes Lépidoptères. Société des Sciences Naturelles de l'Ouest de la France, Nantes, 296 pp.

Gerasimov AM (1935) Zur Frage der Homodynamie der Borsten von Schmetterlingsraupen. Zoologischer Anzeiger 112: 177–194.

Gogoi B, Goswami BC (2016) Silkworm bio-diversity of Assam: Its exploration and development. International Journal of Interdisciplinary Research in Science Society and Culture 2(1): 400–407.

Gogoi H, Borah G, Habung T, Wangsa K (2014) A field survey of the silk moths (Lepidoptera: Saturniidae) in West Siang district, Arunachal Pradesh and threats to their population. Journal of Bioresources 1(1): 16–24.

Goossens R, Meert R, Pollet M (2015) Breeding report of *Antheraea godmani* (Lepidoptera: Saturniidae).

Grimes LR, Neunzig HH (1986a) Morphological survey of the maxillae in last stage larvae of the suborder Dytrisia (Lepidoptera): Palpi. Annals of the Entomological Society of America 79(3): 491–509. https://doi.org/10.1093/aesa/79.3.491

Grimes LR, Neunzig HH (1986b) Morphological survey of the maxillae in last stages larvae of the suborder Ditrysia (Lepidoptera): Mesal lobes (laciniogaleae). Annals of the Entomological Society of America 79(3): 510–526. https://doi.org/10.1093/aesa/79.3.510

Gupta IJ (2000) Insceta: Lepidoptera: non-malberry silkmoths [*sic*]. In: Alfred JRB (Ed.) State Fauna Series 4: Fauna of Meghalaya, Part 5. Zoological Survey of India, Calcutta, 421–435.

Gupta ML, Narang RC (1981) Karyotype and meiotic mechanism in Muga silkmoths, *Antheraea compta* Roth. and *A. assamensis* (Helf.) (Lepidoptera: Saturniidae). Genetica 57(1): 21–27. https://doi.org/10.1007/BF00057539

Hall DW (2021) Polyphemus Moth *Antheraea polyphemus* (Cramer) (Insecta: Lepidoptera: Saturniidae: Saturniinae). Ask IFAS: EENY-531.

Hasenfuss I, Kristensen NP (2003) Skeleton and muscles: immatures. In: Kristensen NP (Ed.) Handbook of Zoology (Vol. 4), Arthropoda: Insecta, Part 36: Lepidoptera: Moths and Butterflies (Vol. 2): Morphology, Physiology, and Development. Walter de Gruyter, Berlin-New York, 133–164. https://doi.org/10.1515/9783110893724.133

Heinrich C (1916) On the taxonomic value of some larval characters in the Lepidoptera. Proceedings of the Entomological Society of Washington 18(3): 154–164.

Heppner JB, Wang HY (1987) Morphology of the larva of *Rhodinia verecunda* Inoue (Lepidoptera: Saturniidae) in Taiwan. Journal of Taiwan Museum 40(2): 33–39.

Hinton HE (1946) On the homology and nomenclature of the setae of lepidopterous larvae, with some notes on the phylogeny of the Lepidoptera. Transactions of the Royal Entomological Society of London 97(1): 1–37. https://doi.org/10.1111/j.1365-2311.1946.tb00372.x

Hipp AL, Manos PS, Hahn M, Avishai M, Bodénès C, Cavender-Bares J, Crowl AA, Deng M, Denk T, Fitz-Gibbon S, Gailing O, González-Elizondo MS, González-Rodríguez A, Grimm GW, Jiang XL, Kremer A, Lesur I, McVay JD, Plomion C, Rodríguez-Correa H, Schulze ED, Simeone MC, Sork VL, Valencia-Avalos S (2019) Genomic landscape of the global oak phylogeny. The New Phytologist 226(4): 1198–1212. https://doi.org/10.1111/nph.16162

Huang CJ, Zhang YT, Bartholomew B (1999) Fagaceae. In: Wu ZY, Raven PH (Eds) Flora of China (Vol. 4) (Cycadaceae through Fagaceae). Science Press, Beijing, Missouri Botanical Garden Press, St. Louis, 314–400.

Jolly MS (1981) Distribution and differentiation in *Antheraea* species (Saturniidae: Lepidoptera). In: Sakate S, Yamada H (Eds) Study and Utilization of non-Mulberry Silkworms, Symposium of XVI International Congress of Entomology, August 3–9, 1980, Kyoto, Japan, 14 pp.

Kakati LN, Chutia BC (2009) Diversity and ecology of wild sericigenous insects in Nagaland, India. Tropical Ecology 50(1): 137–146.

Kalita T, Dutta K (2014) Biodiversity of Sericigenous insects in Assam and their role in employment generation. Journal of Entomology and Zoology Studies 2(5): 119–125.

Keil TA (1999) Morphology and development of the peripheral olfactory organs. In: Hansson BS (Ed.) Insect Olfaction, Springer, Berlin-Heidelberg, 5–57. https://doi.org/10.1007/978-3-662-07911-9_2

Keisa TJ, Luikham R, Singh S, Vijayakumari KM (2022) Biodiversity of wild silkmoths in north eastern india. Plant Archives 22, Special Issue (VSOG): 45–49. https://doi.org/10.51470/PLANTARCHIVES.2022.v22.specialissue.010

Kumar R, Chutia P, Ahmed M, Rajkhowa G, Singh NI (2016) Checklist of wild silk moths of North East India (Lepidoptera: Saturniidae, Bombycidae). Munis Entomology & Zoology 11(2): 508–514.

Kumar D, Shrivastava S, Gong CL, Shukla S (2020) Silk: an amazing biomaterial for future medication. In: Kumar D, Shahid M (Eds) Natural Materials and Products from Insects: Chemistry and Applications, Springer, Cham, 39–49. https://doi.org/10.1007/978-3-030-36610-0_3

Lahiri S, Das M, Mukherjee A (2017) A contribution to the study of *QUERCUS* L. in the Himalayas. Indian Journal of Scientific Research 7(2): 15–20.

Lalhmingliani E (2015) Biodiversity and molecular phylogeny of wild silk moths in Mizoram based on 16s rRNA and CO1 gene markers. PhD Thesis, Department of Zoology Mizoram University, Aizawl, India.

Lampe REJ (2010) Saturniidae of the World (Pfauenspinner der Welt). Verlag Dr. Friedrich Pfeil, München, 368 pp.

Lemaire C (1978) Les Attacidae Americains. The Attacidae of America (= Saturniidae). Attacinae. Édition C. Lemaire, Neuilly-sur-Seine, 238 pp. [49 pls.]

Luikham R, Keisa TJ, Bidyapati L, Sinha AK, Peigler RS (2017) Biodiversity of sericigenous saturniidae of Manipur in India. Munis Entomology & Zoology 12(2): 500–507.

Marepally L (2018) Tasar Culture. Educreation Publishing, New Delhi, 84 pp.

Meister F (2011) A Guide to the Breeding of Tropical Silk Moths (Lepidoptera: Saturniidae). Verlag Dr. Friedrich Pfeil, München, 220 pp.

Menitsky YL (2005) Oaks of Asia (Translated from Russian). Science Publishers, Inc., Enfield, 549 pp.

Nässig WA (1989) Wehrorgane und Wehrmechanismen bei Saturniidenraupen (Lepidoptera, Saturniidae). Verhandlungen des Westdeutschen Entomologentag Düsseldorf 1988: 253–264.

Nässig WA (1991) New morphological aspects of *Antheraea* Hübner and attempts towards a reclassification of the genus (Lepidoptera, Saturniidae). Wild Silkmoths 1989/1990: 1–8.

Nässig WA, Lampe REJ, Kager S (1996) The Saturniidae of Sumatra (Lepidoptera) [+ Appendix I]. In: Nässig WA, Lampe REJ, Kager S (Eds) Heterocera Sumatrana Volume 10 (8th of the "Green Book Series"). Heterocera Sumatrana Society, Göttingen, 3–170.

Naumann S, Löffler S (2015) A new species of the genus *Antheraea* Hübner, 1819 ("1816") from Tibet (Lepidoptera: Saturniidae). The European Entomologist 7(1): 15–26.

Naumann S, Nogueira GG (2021) A new species of the genus *Antheraea* Hübner from the Sierra Madre del Sur, Mexico (Lepidoptera: Saturniidae). The European Entomologist 13(2): 3–17.

Negi SS, Naithani HB (1995) Oaks of India, Nepal and Bhutan. International Book Distributors, Dehradun, 266 pp.

Packard AS (1914) Memoirs of the National Academy of Sciences 12 (1st Memoir): Monograph of the Bombycine Moths of North America, Including Their Transformations and Origin of the Larval Markings and Armature. Part 3. Families Ceratocampidae (Exclusive of Ceratocampinae), Saturniidae, Hemileuciidae, and Brahmaeidae (Edited by Cockerell TDA). National Academy of Sciences, Washington, 516 pp. [113 pls.] https://doi.org/10.5962/bhl.title.8961

Paukstadt U, Suhardjono, Paukstadt LH (2003) Notes on the distribution of the genus *Antheraea* Hübner, 1819 ("1816") and of some selected hosts of the larvae of this genus in the Indonesian Archipelago (Lepidoptera: Saturniidae). Galathea. Berichte des Kreises Nürnberger Entomologen eV, Supplement 14: 25–64.

Paukstadt U, Paukstadt LH (2020) Die Zucht von *Antheraea* (*Telea*) *montezuma* (Sallé, 1856) oder eines nah verwandten Taxons aus Durango, Mexiko (Lepidoptera: Saturniidae). Beiträge zur Kenntnis der Wilden Seidenspinner 18(7): 271–305.

Paukstadt U, Brosch U, Paukstadt LH (2000) Preliminary checklist of the names of the worldwide genus *Antheraea* Hübner, 1819 ("1816") (Lepidoptera: Saturniidae). Part 1. Galathea. Berichte des Kreises Nürnberger Entomologen eV, Supplement 9: 1–59.

Pease RW (1960) A study of first instar larvae of the Saturniidae, with special reference to Nearctic genera. Journal of the Lepidopterists Society 14(2): 89–111.

Peigler RS (1993) Wild silks of the world. American Entomologist (Lanham, Md.) 39(3): 151–162. https://doi.org/10.1093/ae/39.3.151

Peigler RS (1999) Taxonomy, distribution, and sericultural potential of the American species of *Antheraea* (Saturniidae). Bulletin of Indian Academy of Sericulture 3(1): 1–9.

Peigler RS (2020) Wild silks: their entomological aspects and their textile applications. In: Kozłowski RM, Mackiewicz-Talarczyk M (Eds) Handbook of Natural Fibres (Vol. 1): Types, Properties and Factors Affecting Breeding and Cultivation (2nd edn). Woodhead Publishing, Cambridge, 715–745. https://doi.org/10.1016/B978-0-12-818398-4.00021-9

Peterson A (1948) Larvae of Insects, An Introduction to Nearctic Species, Part I: Lepidoptera and Plant Infesting Hymenoptera. Edwards Brothers, Ann Arbor, 315 pp.

Piao MH, Lee CY (1998) Description of the taxonomic terminology of Lepidoptera larvae. Journal of Forest and Environmental Science 14(1): 14–23.

Rothschild W, Jordan K (1899) On some new Lepidoptera from the east. Novitates Zoologicae 6(3): 429–444.

Rothschild W, Jordan K (1901) On some Lepidoptera. Novitates Zoologicae 8(4): 401–407. [pls. 9–10] https://doi.org/10.5962/bhl.part.22170

Rougerie R, Estradel Y (2008) Morphology of the preimaginal stages of the African emperor moth *Bunaeopsis licharbas* (Maassen and Weyding): Phylogenetically informative characters within the Saturniinae (Lepidoptera: Saturniidae). Journal of Morphology 269(2): 207–232. https://doi.org/10.1002/jmor.10562

Rougerie R, Naumann S, Nässig WA (2012) Morphology and molecules reveal unexpected cryptic diversity in the enigmatic genus *Sinobirma* Bryk, 1944 (Lepidoptera: Saturniidae). PLoS ONE 7(9): e43920. https://doi.org/10.1371/journal.pone.0043920

Ryan MF (2002) Insect Chemoreception Fundamental and Applied. Kluwer Academic Publishers, New York-Boston-Dordrecht-London-Moscow, 330 pp.

Schneider D (1964) Insect antennae. Annual Review of Entomology 9(1): 103–122. https://doi.org/10.1146/annurev.en.09.010164.000535

Schoonhoven LM, Dethier VG (1966) Sensory aspects of host-plant discrimination by lepidopterous larvae. Archives Neerlandaises de Zoologie 16(4): 497–530. https://doi.org/10.1163/036551666X00057

Schüssler H (1933) Lepidopterorum Catalogus Parts 56: Saturniidae 2, Subfam. Saturniinae I (Edited by Strand E). W. Junk, Berlin, 324 pp.

Seidel CL, Peigler RS (2018) Review: Entomological aspects of sericulture based on *Antheraea assamensis* and *Samia ricini* (Saturniidae) in Assam and Meghalaya. Tropical Lepidoptera Research 28(1): 13–18.

Seitz A (1926–1928) 14. Familie: Saturniidae, Nachtpfauenaugen. In: Seitz A (Ed.) (1911–1933) Die Gross-Schmetterlinge der Erde. Eine systematische Bearbeitung der bis jetzt bekannten Gross-Schmetterlinge. Band 10. Die Indo-Australischen Spinner und Schwärmer. A. Kernen, Stuttgart, 497–520. [pls. 52–56A]

Shangpliang JW, Hajong SR (2015a) Diversity, species richness and evenness of wild silk moths collected from Khasi hills of Meghalaya, North East India. Journal of Entomology and Zoology Studies 3(1): 168–173.

Shangpliang JW, Hajong SR (2015b) The wild silk moths (Lepidoptera: Saturniidae) of Khasi Hills of Meghalaya, north east India. International Journal of Plant. Animal and Environmental Sciences 5(2): 20–24.

Shields VDC (2008) Ultrastructure of insect sensilla. In: Capinera JL (Ed.) Encyclopedia of Entomology (2nd edn.). Springer, Dordrecht, 4009–4023. https://doi.org/10.1007/978-1-4020-6359-6_2295

Shubhalaxmi V (2018) Birdwing Field Guide to Indian Moths. Birdwing Publishers, Mumbai, 461 pp.

Singh B, Roy DK, Barbhuiya HA, Daimary R (2009) Note on *Quercus griffithii* Hook. f. & Thomson ex Miq.: An interesting wild economic plant of North-East India. Journal of Non-Timber Forest Products 16(3): 205–206. https://doi.org/10.54207/bsmps2000-2009-69VHOJ

Singh RK, Singh A, Garnett ST, Zander KK, Lobsang, Tsering D (2015) Paisang (*Quercus griffithii*): A keystone tree species in sustainable agroecosystem management and livelihoods in Arunachal Pradesh, India. Environmental Management 55(1): 187–204. https://doi.org/10.1007/s00267-014-0383-y

Sondhi S, Karmakar T, Sondhi Y, Kunte K (2021a) Moths of Tale Wildlife Sanctuary, Arunachal Pradesh, India with seventeen additions to the moth fauna of India (Lepidoptera: Heterocera). Tropical Lepidoptera Research 31(Supplement 2): 1–53.

Sondhi S, Sondhi Y, Roy P, Kunte K (2021b) Moths of India, v. 2.71. Indian Foundation for Butterflies. https://www.mothsofindia.org

Stehr FW (1987) Order Lepidoptera. In: Stehr FW (Ed.) Immature Insects. Kendall Hunt Publishing, Dubuque, 288–305.

Tuskes PM, Tuttle JP, Collins MM (1996) The Wild Silk Moths of North America: A Natural History of the Saturniidae of the United States and Canada. Cornell University Press, Ithaca-London, 250 pp. [30 pls.] https://doi.org/10.7591/9781501738005

Watson JH (1912) The wild silk moths of the world, with special reference to the Saturnidae [*sic*]. Manchester School of Technology, Manchester, 8 pp. [4 pls.]

Yang N, Zhou XW (2015) Motuo Zhiwu [Plants of Mêdog]. China Forestry Publishing House, Beijing, 232 pp. [in Chinese]

Zacharuk RY, Shields VD (1991) Sensilla of immature insects. Annual Review of Entomology 36(1): 331–354. https://doi.org/10.1146/annurev.en.36.010191.001555

Zhou ZK, Sun H (1996) A revision of Fagaceae from Tibet. Acta Botanica Yunnanica 18(2): 211–225.

Zhou ZK, Sun H, Yu HY (1995) Distribution of Fagaceae in Tibet. Acta Botanica Yunnanica 17(2): 144–152.

Supplementary material 1

Feeding schedule of *Antheraea compta* L_6

Author: Zhengyang Liu
Data type: table (.xlsx file)
Copyright notice: This dataset is made available under the Open Database License (http://opendatacommons.org/licenses/odbl/1.0). The Open Database License (ODbL) is a license agreement intended to allow users to freely share, modify, and use this Dataset while maintaining this same freedom for others, provided that the original source and author(s) are credited.
Link: https://doi.org/10.3897/dez.70.102952.suppl1

Supplementary material 2

Light sensitivity (the darker side = ca. 544-1185 Lux, the brighter side = ca. 9300-13600 Lux) of *Antheraea compta* L_6 (speed × 12)

Author: Zhengyang Liu
Data type: video (.mov file)
Copyright notice: This dataset is made available under the Open Database License (http://opendatacommons.org/licenses/odbl/1.0). The Open Database License (ODbL) is a license agreement intended to allow users to freely share, modify, and use this Dataset while maintaining this same freedom for others, provided that the original source and author(s) are credited.
Link: https://doi.org/10.3897/dez.70.102952.suppl2

Supplementary material 3

Defensive behavior of *Antheraea compta* L_6

Author: Zhengyang Liu
Data type: video (.mov file)
Copyright notice: This dataset is made available under the Open Database License (http://opendatacommons.org/licenses/odbl/1.0). The Open Database License (ODbL) is a license agreement intended to allow users to freely share, modify, and use this Dataset while maintaining this same freedom for others, provided that the original source and author(s) are credited.
Link: https://doi.org/10.3897/dez.70.102952.suppl3